JOHANNES KEPLER
UNIVERSITÄT LINZ | JKU

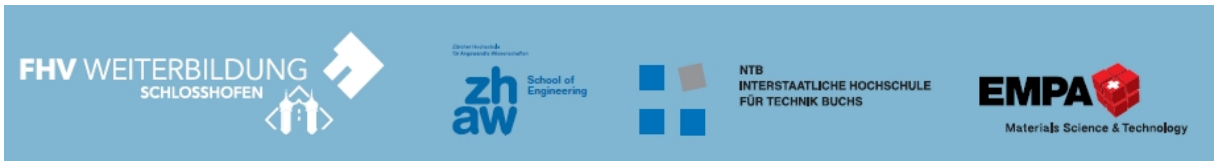

Measurement of charge carrier mobility and charge carrier concentration of organic photovoltaic diodes under in situ light soaking conditions and varying temperatures

MASTERARBEIT

zur Erlangung des akademischen Grades

Master of Science MSc

im Masterstudium

Micro- and Nano Technology

Eingereicht von:
Stefan Kraner

Personenkennzeichen:
0819003015

Angefertigt am:
Institut für physikalische Chemie in Linz

Beurteilung:
Mag.Dr.o.Univ.-Prof. Serdar N. Sariciftci
Prof. Dr. Beat Ruhstaller

Betreuung:
Dr. Matthew White

Linz, 24. Mai 2011

Eidesstattliche Erklärung

Ich erkläre an Eides statt, dass ich die vorliegende Masterarbeit selbstständig und ohne fremde Hilfe verfasst, andere als die angegebenen Quellen und Hilfsmittel nicht benutzt bzw. die wörtlich oder sinngemäß entnommenen Stellen als solche kenntlich gemacht habe.

Linz, am 24. Mai 2011

Stefan Kraner

Kurzfassung

In dieser Arbeit wurde die Ladungsträgerkonzentration, die Ladungsträgermobilität und die Leitfähigkeit von Poly(3-hexylthiophene-2,5-diyl) (P3HT) Dioden und P3HT-PCBM (Phenyl-C61-butyric acid methyl ester) bulk heterojunction (BHJ) Solarzellen gemessen. P3HT:PCBM ist ein weit verbreitetes OPV Materialsystem. Die Messungen wurden bei verschiedenen Temperaturen und variierender Beleuchtung durchgeführt. Die Mobilität wurde mit der CELIV- (charge extraction by linear increasing voltage) und mit der space charge limited current (SCLC) Methode bestimmt, während die Ladungsträgerkonzentration mit CELIV und über eine Impedanzmessung (Mott-Schottky Diagram) gemessen wurde. Die Leitfähigkeit konnte mit einer abgewandelten 4 Punkte Messung ermittelt werden.

In der P3HT Diode haben die Mobilitätsmessungen mit CELIV oder SCLC ähnliche Resultate ergeben. Durch eine permanente Beleuchtung des Filmes erhöht sich die Mobilität geringfügig. Gegenüber der Ladungsträgerkonzentration im Dunkeln, ist sie bei permanenter Beleuchtung mit einer Lichtintensität von 5 mW/cm^2 (ca. 5 % der Strahlungsleistung der Sonne) mehr als doppelt so gross. Wird die Lichtintensität weiter erhöht, bleibt wegen den fehlenden Akzeptormolekülen die Ladungsträgerkonzentration in der P3HT Diode konstant. Die Konsistenz der Messungen wurde mit der Formel $\sigma = en\mu$ überprüft (σ = Leitfähigkeit, e = Elementarladung, n = Ladungsträgerkonzentration, μ = Mobilität). Die gemessene Leitfähigkeit stimmt gut mit der berechneten Leitfähigkeit überrein. Die 2 bis 5 mal höhere gemessene Leitfähigkeit kann teilweise auf die unterschiedlichen verwendeten Geometrien der Filme zurückgeführt werden.

In der P3HT-PCBM BHJ Solarzelle haben die Mobilitäten, gemessen mit CELIV und SCLC, ähnliche Werte. Zwei Solarzellen, eine wurde innerhalb und die andere ausserhalb der Glovebox rotationsbeschichtet, haben ein unterschiedliches Verhalten der Mobilität. Wird der Film in der Glovebox beschichtet, erhöht sich, wie beim P3HT Film, bei steigenden Temperaturen oder Lichtintensitäten auch die Mobilität. Wird der P3HT-PCBM Film ausserhalb der Glovebox beschichtet, und dadurch dem Sauerstoff exponiert, führen höhere Lichtintensitäten zu niedrigeren Mobilitäten. Erhöht man die Lichtintensität auf die Solarzelle steigt die Ladungsträgerkonzentration, da die erzeugten Ladungsträger separiert werden können. Mit einer Beleuchtung und bei einer maximaler Effizienz der Solarzelle, ist die berechnete Dicke der Verarmungszone gleich Null. Damit befindet sich die Absorberschicht nicht im elektrischen Feld der Verarmungszone. Dies wiederum unterstützt die Annahme, dass der Ladungsträgertransport in einer Solarzelle vom Diffusionsstrom dominiert wird. Im Dunkeln ist die berechnete und gemessene Leitfähigkeit unerklärlicherweise stark unterschiedlich. Mit einer Beleuchtung von 5 mW/cm^2 stimmt die gemessene Leitfähigkeit gut mit der berechneten Leitfähigkeit überrein.

Abstract

Charge carrier mobility, charge carrier concentration and conductivity were measured on a Poly(3-hexylthiophene-2,5-diyl) (P3HT) diode and on a P3HT-PCBM (Phenyl-C61-butyric acid methyl ester) bulk heterojunction (BHJ) device. P3HT:PCBM is a commonly used material system in organic photovoltaic (OPV) devices. The measurements were done at different temperatures and varying light conditions. The mobility of the charge carriers was measured with the charge extraction by linear increasing voltage (CELIV) and with the space charge limited current (SCLC) method. The charge carrier concentration was measured by CELIV and impedance (Mott-Schottky plot). The conductivity was measured by a modified 4 wire conductivity technique.

The mobility in a P3HT device measured by CELIV and SCLC gives similar results. Permanent illumination does slightly increase the mobility. Compared to the dark, the charge carrier concentration in a P3HT device more than doubles with a small light intensity of 5 mW/cm^2 (ca. 5 % of one sun). Due to the missing acceptor molecules (PCBM), further increasing the light intensity does not increase the charge carrier concentration anymore. To check the consistency of the different measurements equation $\sigma = en\mu$ (σ=conductivity, e =elementary charge, n =charge carrier concentration, μ=mobility) was used to calculate the conductivities. The measured conductivities at different temperatures are in a good agreement with the calculated conductivities. The 2 to 5 times higher measured conductivitiy could partially be attributed to the different device geometries.

In the P3HT-PCBM BHJ solar cell (SC) the mobility, measured by SCLC and CELIV, is in a similar range. Two solar cells, one spin coated in the glovebox, the other outside the glovebox, have an opposite mobility behavior. Spin coating inside the glovebox leads to the same mobility behavior as in the P3HT device, higher temperature or higher light intensity induces higher mobility. The solar cell, spin coated outside the glovebox, and thus is more exposed to oxygen, acts opposite regarding illumination behavior. Higher light intensity induces lower mobility. Since photo generated charges are separated in the OPV device, irradiance of 5 mW/cm^2 generates 5-10 times more charges than in the dark and increases with higher light intensities. The calculated depletion layer thickness under illumination and at the maximum power point of the SC is zero. Thus the bulk is not affected by the electric field of the depletion layer. This may support the idea, that the charge transport in an OPV device is diffusion dominated. The calculated conductivities in the dark are 50-80 times lower than the measured conductivities, which can not be explained. With 5 mW/cm^2 light intensity the measured conductivities are in a good agreement with the calculated conductivity, like in the P3HT device.

Acknowledgment

I want to thank all the members of the LIOS group for the support during my stay at LIOS. Special thanks go to my supervisor Dr. Matthew White, who always took time to answer my questions and also introduced me in the lab and with the lab equipment. I also want to thank Prof.N.S. Sariciftci, who gave me the opportunity to work at LIOS and gain experience from the knowledge of his group.

Special thanks go also to European Science Foundation (ESF) for funding this work within the activity entitled: New Generation of Organic based Photovoltaic Devices.

Contents

Chapter 1

Introduction

1.1 Motivation

Efficient harvesting of solar energy is one of the great scientific and industrial challenges of today. Environmental, social, and economic factors all motivate this push.

Organic solar cells are a promising possibility to achieve low production cost and extremely high production rates. Organic solar cells are either based on small molecules or polymers. Both technologies can be processed on plastic as a substrate. This reduces the production costs, and since the active layer is only a few hundred nanometers thick, it does not affect the overall price significantly. Polymer based solar cells can be produced with solution process technologies. High speed production similar to newspaper production lines are possible. The highest efficiency of 8.3 % was achieved from Konarka Technologies Inc. in 2011. Nevertheless, the efficiency is still far below the inorganic solar cells with efficiencies up to 42.8 %, achieved by two scientists at the University of Delaware. The disadvantage of the organic solar cells is the low efficiency and the limited long term stability.

In the field of polymer solar cells the bulk heterojunction is the current design to achieve the highest efficiencies with organic films. In this thesis, the current laboratory standard materials used in bulk heterojunction OPV devices are investigated. Several different techniques are used to characterize charge carrier concentration, mobility and the overall conductivity under varying temperature and light conditions. Using multiple techniques allows for independent confirmation of the results, and furthermore to check the consistency between the different measurement systems. A thorough understanding of the temperature and illumination dependence of the charge carrier behavior helps clarify how the devices function, and what can be done to improve them, in order to get higher efficiencies.

1.2 Theoretical background

1.2.1 Bulk heterojunction solar cell

A bulk heterojunction solar cell consists of an active organic part with a donor and an acceptor material, the metal electrodes and the substrate [1]. The substrate is responsible for mechanical stability and also should protect the organic material from moisture. Usually the substrate is transparent, so the light will first pass the substrate before it reaches the active material. The material of the substrate is usually glass, but it could also be a transparent plastic. There are two electrodes, a positive and a negative. The positive electrode in the figure 1.1(a) is indium tin oxide (ITO). ITO is transparent, and good conductive material. The aluminum represents the negative electrode. The aluminum electrode is thick enough to reflect the unabsorbed light back into the device. Both electrodes have the task to transport the charges from the organic material to the electrical connections with minimal losses. The level of the electrode work functions can be optimized for electron and hole extraction to selectively design a quality diode. If the work functions do not fit, it is possible to introduce an additional layer between the electrode and the organic material to adjust the work functions of the different materials. That's one of the tasks from Poly(3,4-ethylenedioxythiophene):Polysytrenesulphonat (PEDOT:PSS). Also, intermediate layers can block the transport of holes or electrons.
Finally, in the middle of the solar cell, the organic part is present. The organic donor and acceptor materials have different electron affinities, which means that the acceptor material rather receives electrons than releases. Whereas the donor material prefers to release electrons. The acceptor material in the presented example is PCBM. P3HT is the donor material. It absorbs most of the light in a bulk heterojunction solar cell.

The working principle of an bulk heterojunction solar cell is showed in figure 1.1(b). If the incoming photon has an equal or higher energy than the optical bandgap in the absorber material, then there is a probability for the photon to be absorbed. The optical bandgap is defined by the difference of the band levels of the highest occupied molecular orbital (HOMO) and lowest unoccupied molecular orbital (LUMO) of the absorber material (P3HT). If the photon is absorbed, an exciton is generated. An exciton is a quasi neutral particle and contains a positive and negative charge. An exciton can diffuse maximum 20nm in its lifetime [2]. If the exciton does not reach the donor acceptor interface it will recombine, and the absorbed energy is converted into thermal energy or as an emitted photon and cannot be used for power generation. If the exciton reaches the interface it can dissociate, with the electron transferring to the acceptor material. Some energy is lost due to the difference in the LUMO levels of the donor and acceptor material. The generated charges are driven by drift and diffusion to the electrodes, where they are free to move through the external circuit.
In inorganic solar cells the absorber material generates free charges, since the dielectric constant of the absorber material ($\epsilon_{Si} = 11$) is much higher compared to the organic absorber material ($\epsilon_{P3HT} = 3$). In OPV devices an acceptor and a donor material is needed to generate free charges. In a pure absorber material, excitons would be generated but not separated and therefore no photo generated charges should be visible. In this case excitons are only able to separate at impurities. This will be discussed in relation to the measurements in this thesis.

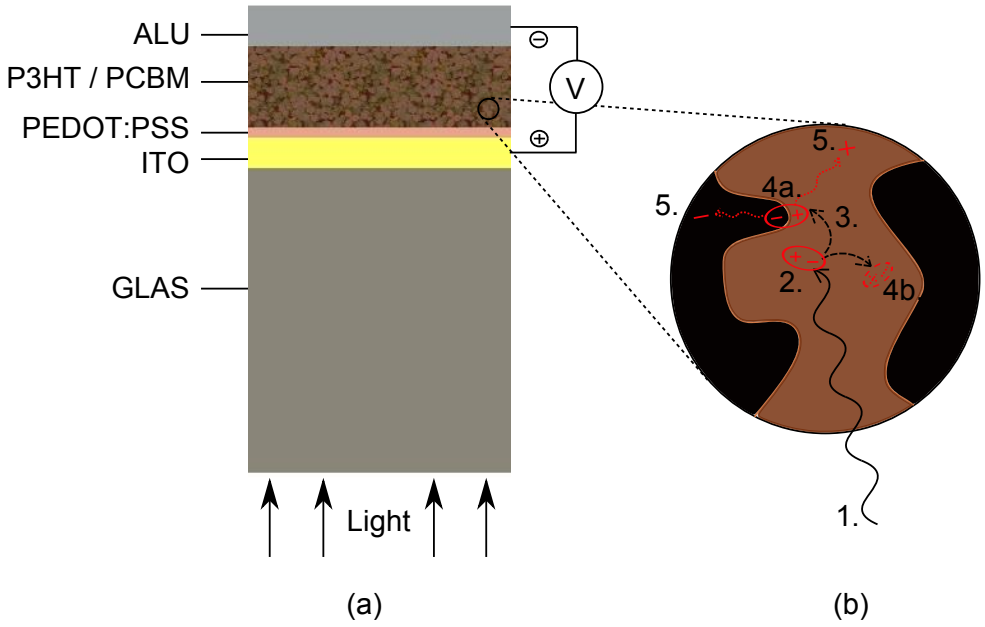

Figure 1.1: a) Intersection of a bulk heterojunction solar cell. b) Concept of the functionality of an organic solar cell: 1.Light with energy $E = h\nu$, 2.Exciton generation, 3.Exciton diffusion, 4a.Exciton dissociation, 4b.Exciton recombination, 5.Charge drift and diffusion to specific electrodes

According to the diffusion length of about 20 nm, the donor and acceptor material should interpenetrate each other in the nanometer scale, to keep a low probability for the recombination of the exciton. The separated charges also have a lifetime. If the thickness of the film is too high, the charges will recombine before they reach the electrodes. Therefore, the thickness of the device is limited by the mobility of the carriers in the organic semiconductor. In thin devices, on the other hand, many photons are not absorbed. Thus, there is a optimum to find, between high absorption rate and low recombination rate for separated charges. The system can be optimized by increasing the carrier mobility [3] and the optical absorption coefficient of the materials.

1.2.2 Space charge limited current

With the space charge limited current (SCLC) method, one can calculate the mobility of a organic semiconductor with a simple IV curve. The SCLC is a description of a behavior of the voltage dependence on the current in a semiconductor. SCLC occurs when the charge carrier concentration is larger than the doping level or the free carriers in a semiconductor. This can happen by injecting charge carriers into the device. This current is dominated by the applied field, what one calls a drift current. The high charge carrier concentration affects the electric field distribution, which makes a feedback loop between the field and the current. This feedback mechanism is described in the relation 1.1 and is called the Mott-Gurney law.

$$J = \frac{9\varepsilon_s \mu V^2}{8L^3} \tag{1.1}$$

V is the applied voltage, J the SCLC, L is the thickness of the film, μ the mobility and ε_s is the permittivity of the semiconductor. It has been shown that SCLC can also be used for mobility measurement of organic diodes [4]. It is under discussion, that the mobility μ depends on the electric field [5], which is not considered in the Mott-Gurney law. In this thesis the original Mott-Gurney law will be used for comparison to the other techniques.

1.2.3 4 wire conductivity

A modified 4 wire conductivity measurement technique is used in this thesis to measure the conductivity of a thin film. Here the standard 4 wire technique will be introduced.

In order to measure a device accurately, it is important to make sure that the measured physical properties are independent of the used setup. The simplest way to measure the resistance (R) of a device is with 2 contacting wires. By sourcing a current (I) one can measure the voltage (V). After Ohms law $R = \frac{V}{I}$ the resistance can be calculated. 2 wire conductivity measurements can be accurate, but there are some issues.

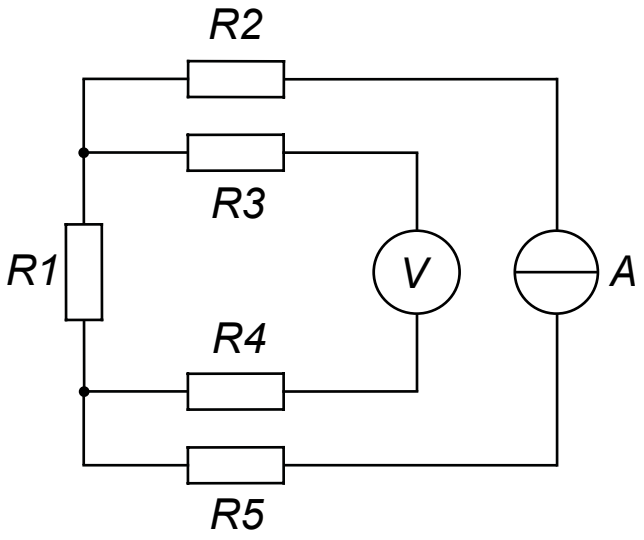

Figure 1.2: Electrical equivalent circuit of a 4 wire conductivity measurement

Figure 1.2 shows an equivalent circuit diagram of a 4 wire setup. $R1$ represents the resistance of interest. $R2$ and $R5$ includes the resistances of the cables to the current source A and the contact resistances from the wire to the devices. $R3$ and $R4$ refer also to the resistances of the contacts to the device and the cables to the voltage meter. In order to measure the resistance $R1$, the power supply (A) should regulate the sourced current accurately. This would make the voltage over the device independently of $R2$ and $R5$. To measure to voltage drop over $R1$ independently of $R3$ and $R4$, the internal resistance of the voltage meter (V) should be infinite. In practice one can choose a voltage meter with a very high internal resistance or at least much higher than $R1$. With this configuration the calculated value of $R1$ is almost independent of $R2 - R5$, which is the purpose and advantage of the 4 wire conductivity measurement.

$$\frac{1}{\rho} = \sigma = en\mu \tag{1.2}$$

In equation 1.2 it is shown, that the reciprocal value from the resistivity (ρ) is the conductivity (σ). The conductivity depends on the charge carrier concentration (n) and on the mobility (μ) of charge carriers itself. By measuring σ, n and μ the consistency of the used measurement methods can be proven, since e is the elementary charge and thus constant.

1.2.4 Impedance measurements

The impedance of a device can be investigated by applying a small signal AC voltage in addition to a DC bias. This allows for the full, frequency dependent, characterization of the resistances, capacitances and inductances that may be acting within the device.
A resistance does not depend on the applied frequency. If a device does have a capacitive or inductive behavior the measured impedance depends on the applied frequency of the voltage. This dependence is readable in the phase shift between the voltage and the current signal. Mathematically this additional information is included in a complex number, which is the impedance (Z). In formula 1.3 θ is the angle between voltage and current signal. R is the real part of the complex number and the resistance, X the reactance, and V and I here also refer to voltage and current but in a complex number.

$$Z = |Z|e^{j\theta} = R + jX = \frac{V}{I} \tag{1.3}$$

$$Zc = \frac{1}{j\omega C} \tag{1.4}$$

Formula 1.4 reflects the impedance of an ideal capacitor. Where $\omega = 2\pi f$ is the angular frequency of the alternating current and C the capacitance. The advantage of the complex numbers are, *Ohm's* and *Kirchhoff's* law can also be used, not only in direct current (DC), but also in alternating current (AC).

Measuring the impedance is typically done frequency dependent, and is then called impedance spectroscopy. But it can also be done at different bias voltages. This means, one applies a DC offset on the device and modulate on the bias a small alternating voltage, which gives the information of the impedance at a specific bias (or offset) voltage. In this thesis diodes will be measured. Diodes have non linear IV characteristic and it is possible to interpret and find out different physical parameters by varying the frequency or bias of the applied voltage.

1.2.4.1 Impedance spectroscopy

As mentioned, in impedance spectroscopy the impedance is measured at various frequencies. The interpretation of the measured results can be done in different ways. Here we interpret

the results by fitting the measured values with a theoretical equivalent circuit. This circuit can contain resistors and capacitors. It has to be mentioned, that infinite equivalent models can reflect the same impedance behavior. To interpret the measured results it makes sense that the equivalent circuit model has components with a physical meaning to the the device under test.

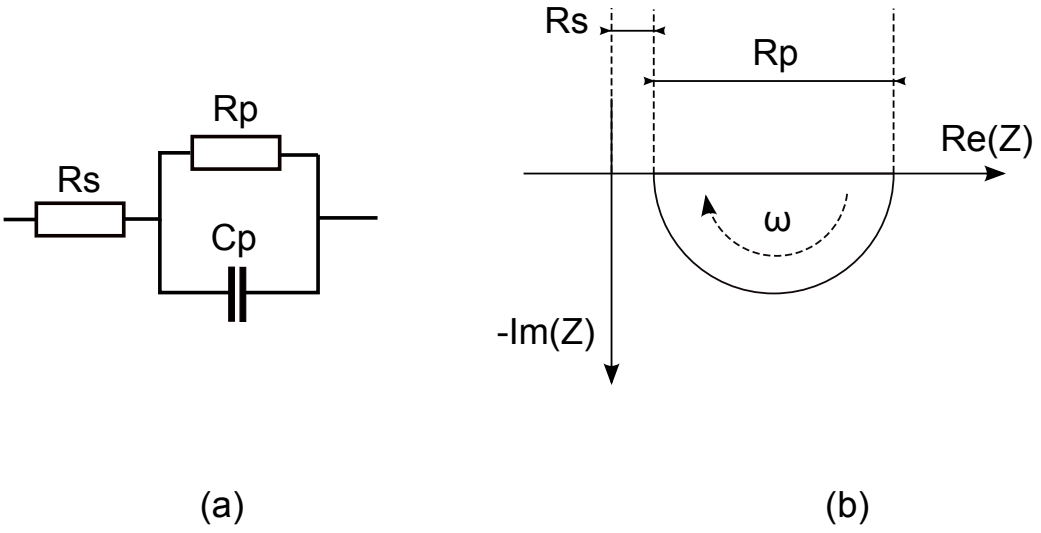

Figure 1.3: (a) example for an equivalent curcuit. (b) Nyquist diagram of the equivalent circuit

In figure 1.3(a) an equivalent circuit diagram is shown with a series resistor (Rs), parallel resistor (Rp) and a parallel capacitor (Cp). The impedance spectrum of this circuit is shown in figure 1.3(b), as the so called Nyquist diagram, where the x axis is the real part and the y axis is the imaginary part of the complex impedance. One can read out of this diagram that due to the negative half circle, there is one capacitor in the circuit with a parallel resistor with the value Rp. Since there is a gap between the half circle and the imaginary axis, a series resistor (Rs) which has the size of the gap is present as well. ω is the angular frequency and increases from the right to the left.

1.2.4.2 Mott Schottky plot

A semiconductor has a charge carrier concentration which effects the distribution of the electric fields within the device. If the carrier concentration is within a certain range, then a Schottky contact is formed at a metal-semiconductor interface and a built-in potential is present. Both, the charge carrier concentration (N) and the built-in potential (ψ_{bi}) at a Schottky contact can be measured and calculated. The used theory will be introduced here.

A Schottky contact consist of a metal and a semiconductor. The Fermi level (E_F in figure 1.4(a)) of a p-type semiconductor is lower than the Fermi level of the metal in a Schottky diode. Which means, that the electron energy level with a occupation probability of 50 % in a p-type semiconductor is lower than in the metal. In order to get a Schottky contact with a

n-type semiconductor, the Fermi level of a n-type semiconductor is higher than the Fermi level of the metal. $e\phi_m$ in figure 1.4(a) stays for the workfunction of the metal and is the difference between the Fermi level of the metal and the vacuum level. $e\psi_i$ refers to ionization energy and $e\phi_p$ refers to the difference of the valence band (E_V) and the Fermi level of the semiconductor. e is the elementary charge.

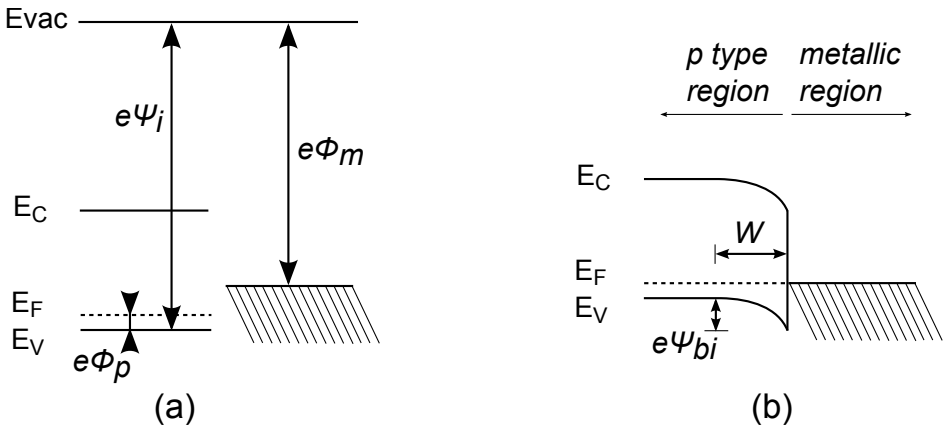

Figure 1.4: Energy band diagram of a p-type Schottky contact. Metal and semiconductor in separated system (a) and in connected system (b).

If there is a contact between the metal and the semiconductor, charges will move across the interface to provide an equilibrium uniform Fermi Level (figure 1.4(b)). In the semiconductor region close to the contact are no mobile charges anymore. This region is called depletion layer and has the width W. This system of a semiconductor and a metal in contact is called a Schottky contact and acts like a diode. By applying a positive voltage on the semiconductor side the depletion layer gets smaller and the current gets higher, this is the so called forward bias. By applying a negative voltage the depletion layer gets bigger, and the current gets smaller, which means, the diode works in the reverse bias regime. The potential difference between the Fermi levels is the contact potential or built-in potential $\psi_{bi} = \psi_i - \phi_m - \phi_p$. The depletion layer width (W) is defined by equation 1.5 [6]:

$$W = \sqrt{\frac{2\varepsilon_s}{eN}\left(\Psi_{bi} - V - \frac{kT}{e}\right)} \tag{1.5}$$

- ε_s: Permittivity of the semiconductor
- V: Applied potential or voltage
- $\frac{kT}{e}$: Correction factor for majority-carrier distribution tails [7].
- k: Boltzmann constant
- N: Charge carrier concentration in the semiconductor

In the following we take a look to the electric field and charge carrier distribution in the film. The material we use in this thesis are organic materials, which do not have to be doped, because the conduction bands or LUMO levels are different in the p-type (donor) and n-type (acceptor) semiconductors, whereby the charge separation is forced. With the assumption, that the intrinsic charges are distributed uniformly, the charge carrier concentration N is constant, see 1.5(a). Based on the Poisson equation 1.6, the integration of the charge carrier concentration gives the electric field (1.5(b)) and the integration of the electric field gives the potential over the film thickness (1.5(c)).

$$-\frac{d^2\psi(x)}{dx^2} = \frac{dE(x)}{dx} = \frac{N(x)}{\varepsilon_s} \tag{1.6}$$

- ψ: Potential
- E: Electric field
- x: Distance perpendicular to the substrate
- N: Charge carrier density

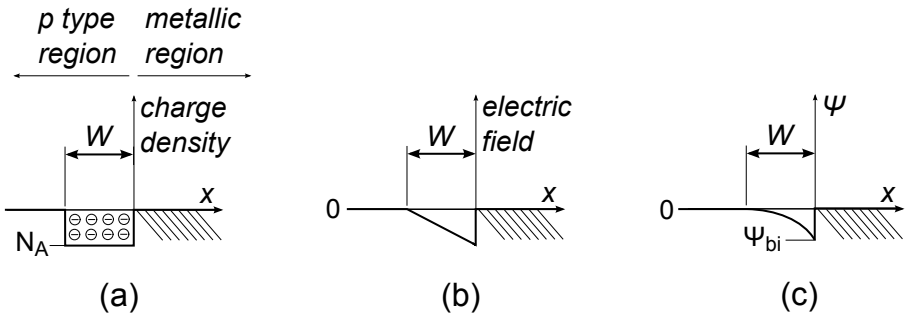

Figure 1.5: Ideal Schottky contact with a depletion layer thickness W, (a) space-charge distribution, (b) electric-field distribution, (c) potential distribution where ψ_{bi} is the built-in potential.

This potential can be used to derive the energy bands (1.4(b)). The derivation for the depletion layer thickness is based on the Poisson equation. In a Schottky diode the metal has a very high charge carrier concentration, and thus one can imagine that the depletion width is very small, almost zero and has not to be considered. However, the depletion layer calculations refer to the semiconductor.

The capacitance (C) can be measured by impedance with various bias voltages. C is calculated from the impedance by an equivalent circuit model with a capacitor and a parallel resistor.

$$C^{-2} = \frac{2(\psi_{bi} - V)}{A^2 e\varepsilon\varepsilon_0 N} \tag{1.7}$$

V is the applied bias voltage and A the area of the capacitor. A series resistance is usually not taken into account, but if one measures Mott Schottky plot at frequencies higher than 100 kHz, corrections need to bee made [8]. Measuring the capacitance over bias voltages showed

in C^{-2} plot gives a straight line, which is a good indication for a present Schottky contact [9]. The extrapolated intersection with the bias axis gives the built-in potential (ψ_{bi}), whereas the slope of the line gives the charge carrier concentration with equation 1.8 which is derived from 1.7.

$$N = -\frac{2}{A^2 e\varepsilon\varepsilon_0 \cdot slope} \tag{1.8}$$

1.2.5 CELIV

Charge extraction by linear increasing voltage (CELIV) is a method to measure charge carrier concentration (N), conductivity (σ) and mobility (μ) [10]. The method can be used for high and low conductive semiconductors. The idea is to apply a linear increasing voltage (V) on the reverse connected device and measure the current response over the time by an oscilloscope (see figure 1.6).

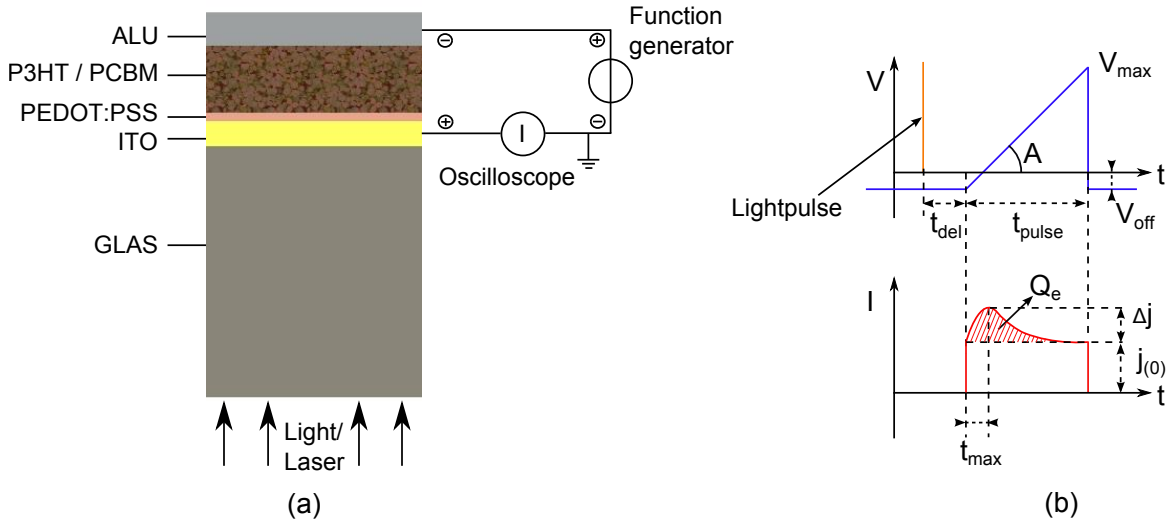

Figure 1.6: CELIV measurement setup. In picture (a): connection diagram. The device is connected in reverse direction to run the diode in reverse bias. (b): the function generator creates the voltage ramp (A) and the oscilloscope measures the current response.

The device needs to have a blocking contact (for example a Schottky contact), otherwise charges are injected and the current pulse is affected or even not visible anymore. If the active organic material would have no free charge carriers, the current response would look rectangular with the height $j_{(0)} = C\frac{V_{max}-V_{off}}{t_{pulse}}$, which represents a capacitive behavior with the geometric capacitance (C) from the diode. Free charges in the active layer begin to move, due to the increasing electric field and are finally extracted at the electrodes. The extracted charges are responsible for the additional peak on $j_{(0)}$, while the time t_{max} gives information about mobility μ (see equation 1.9) of the extracted charges. d is the thickness of the film and Q_e represents the total amount of extracted charges which is the dashed area in figure 1.6(b). With the volume of the film, the charge carrier concentration can be determined.

With formula 1.9 one can calculate the mobility. This formula is valid at low light intensities and with uniformly photo generated charge carriers, which means, an absorption dependence within the film thickness is not considered. Also, equation (1.9) is based on the drift current. A possible diffusion current, specially under illumination, is not considered.

$$\mu = \frac{2d^2}{3At_{max}^2\left[1 + 0.36\frac{\Delta j}{j_{(0)}}\right]} \tag{1.9}$$

The determination of conductivity directly by CELIV will not be used in this thesis.

Chapter 2

Experimental details

2.1 Devices

This chapter introduces the used materials and shows the production procedure of the measured devices.

2.1.1 Materials

2.1.1.1 P3HT

Poly(3-hexylthiophene-2,5-diyl) (P3HT) is a conjugated polymer, see figure 2.1. It is a commonly used polymer in organic solar cells and acts as the light absorbing and hole transporting material. P3HT has a high solubility and due to the alkyl-groups a high potential crystallinity. The degree of crystallinity is affected by the regioregularity of the polymer. A regioregular P3HT usually has a regioregularity of minimum 90 %. The higher the regioregularity, the higher the cristallinity. It was also recognized that higher molecular weight leads to a red shift in the absorbtion spectrum and to higher hole mobility [11][12].

P3HT is a conjugated polymer with a thiophene backbone. The carbon atoms in the thiophene rings are sp2 hybridized, and thus form a π-bond with the neighbor carbon atoms. In the polymer the π-bonds form a π-band which is called the highest occupied molecular orbital (HOMO). In this π-band the electrons are delocalized. The bandgap of thiophenes is build by transition from the aromatic into the quinoid structure. Impurities in the polymer act like a p-type doping and are giving pure P3HT a electrical conductivity.

The used P3HT is from Rieke: 4002-E and has a regioregularity of at least 90 %. The average molecular weight is 50000 g/mol. The LUMO level is 3.2 eV and the HOMO level is at

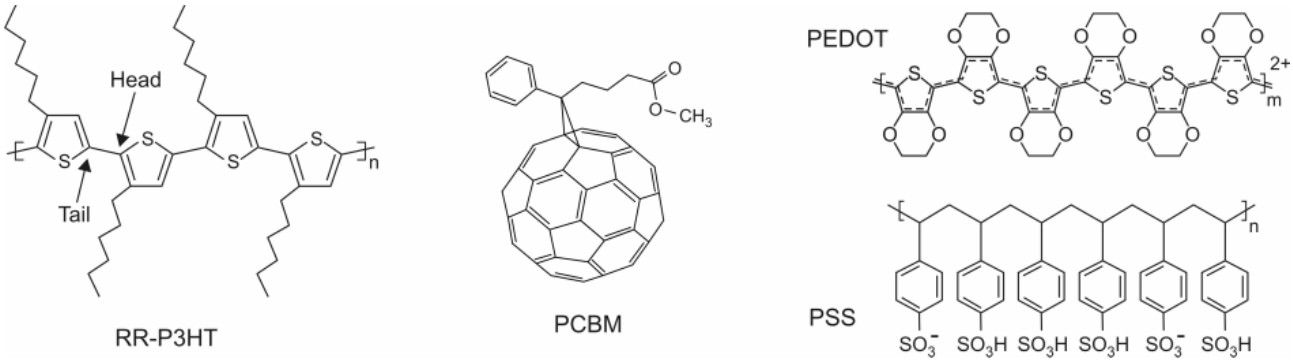

Figure 2.1: Organic molecules used in solar cells: Regioregular P3HT, PCBM, PEDOT:PSS

5.1 eV [13]. The hole mobility in P3HT depends on different factors and lies between 10^{-5} and 10^{-2} cm^2/Vs [5][2]. The electron mobility is negligible small [3].

2.1.1.2 PCBM

Phenyl-C61-butyric acid methyl ester (PCBM) is a fullerene based molecule (figure 2.1). It contains a Bucky-ball (C60), and to make it soluble the methyl-ester group is attached. PCBM is a n-type material and can take up to six electrons. It also has a π-band, but the electrons are moving in the $\pi*$-band, or LUMO. The mobility in PCBM is between $2 \cdot 10^{-3}$ and $2 \cdot 10^{-2}$ cm^2/Vs [3]. The hole mobility is negligible small. The HOMO level is 6.1 eV and the LUMO level is 4.4 eV [13].
In this thesis the PCBM from Solenne 99 % is used.

2.1.1.3 ITO

Indium tin oxide (ITO) is a transparent conductive oxide. In an organic solar cell at least one electrode has to be transparent in order to absorb the light in the active layer. It is quite common in opto-electronics to use ITO. In this thesis the ITO was bought already on the glass from Kintec. It has a sheet resistance of 15 Ω/sq. The work function is 4.9 eV.

2.1.1.4 PEDOT:PSS

$Poly(3,4-ethylenedioxythiophene)$: $Polysytrenesulphonat$ (PEDOT:PSS) is a conducting conjugated polymer (figure 2.1). PEDOT:PSS is used to improve the extraction properties between the ITO and the P3HT and to smooth out the ITO film. The layer thickness is usually less than 100 nm and thus transparent. In this thesis the PEDOT:PSS VP AI 4083 from CLEVIOS is used, which has a work function of 4.8-5.2 eV [14]. The resistivity lies between $500 - 5000$ Ωcm.

2.1.2 Production procedure

The solar cell and the P3HT diode are produced with following procedure. Deviations to the procedure are mentioned in text of the specific devices.

The first step is to cut the glass. Usually the devices at LIOS (Linz Institute for Organic Solar Cells) have a size of about 14 mm x 14 mm x 1 mm. The ITO has to be etched in the area of the aluminum contacts. Therefore the rest of the device has to be protected by a tape. The etching process with a 37 % concentrated HCL (hydrochloric acid) solution takes 5min by an ITO thickness of 150 nm, and the HCL can be reused several times. The next step is to clean the glass. The cleaning process was done in a ultrasonic bath in acetone for 10min and in isopropanol for 10 min. Now the layers can be spin coated on the device. First the PEDOT:PSS is filtered by a PES membrane with 0.45 μm pores and then spin coated twice by a speed of 4000 rpm for 40 s. After removal the PEDOT:PSS with distilled water from the contact areas (figure 2.2(a)) the device has to be annealed at 120 $°C$ for 10 min to remove the residual water in the film.

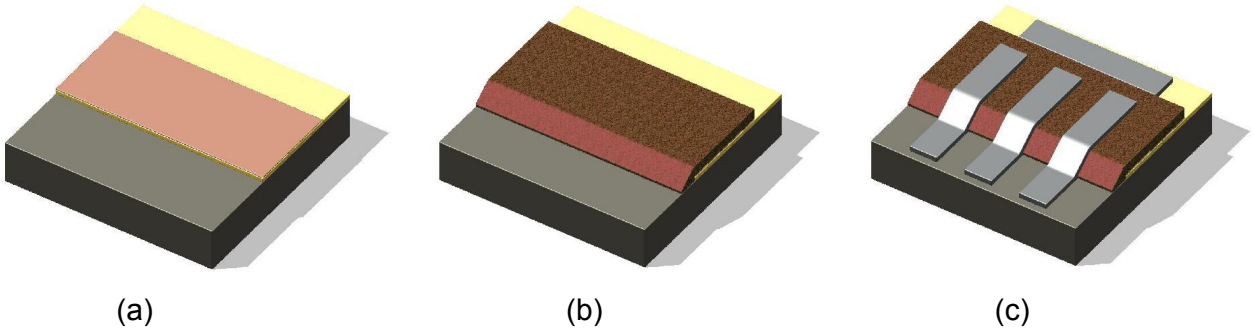

Figure 2.2: Production steps of a device. (a) Spin coat PEDOT:PSS on etched ITO(yellow). (b) Spin coat organic material and remove the edges. (c) Evaporate aluminum electrodes

The organic material for a solar cell contains a mix of PCBM and P3HT. This materials are dissolved in chlorobenzene. The solution concentration lies between 10 and 30 mg/ml. The solutions in this thesis are made with 30 mg/ml, and the mixing ratio between PCBM and P3HT was made 1:1. In order to get a good solution, the mix should be stirred with a stir bar for at least 1h. Now the organic material can be spin coated with a speed between 800 rpm and 1500 rpm. The devices in this thesis are spin coated with 800 rpm. The organic material at the contacts has to be removed as well. This can be done with acetone, toluol or it can be scratched off with a sharp knife. A sharp knife is usually used when the spin coat process was done in the glovebox. In this thesis the organic films are spin coated in the glovebox. Now the aluminum electrodes with a thickness of 100 nm are evaporated. Specially in a solar cell it is important to make a last annealing step to improve the degree of crystallinity in the organic film. The annealing step is done at 120 $°C$ for 10 min. The device is finished (figure 2.2(c)).

2.1.3 P3HT device

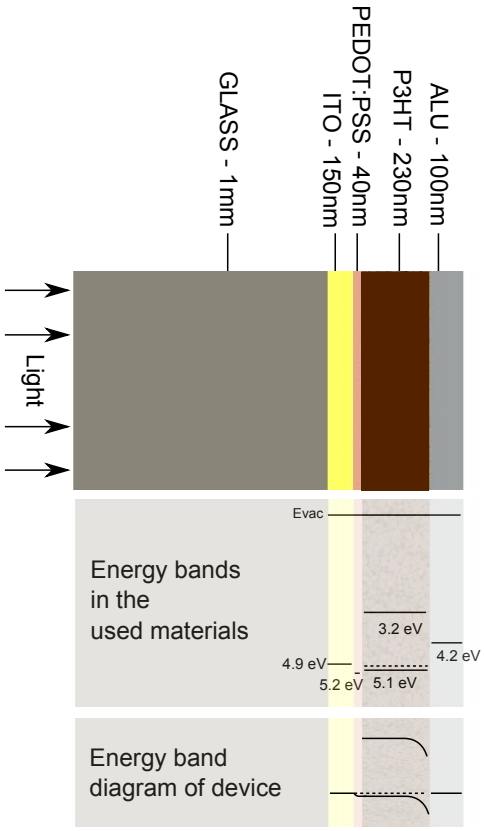

Figure 2.3: Thickness, work functions, electron affinity and energy band diagram of the P3HT device

The device for measurements with pure P3HT is shown in figure 2.3. As a general understanding, PEDOT:PSS on ITO forms an ohmic contact with the P3HT, whereas the P3HT forms a Schottky contact with aluminum and thus has a depletion layer [15]. The energy bands in the P3HT layer show a dotted line, which refers to the p-type doping level. The dotted line in the energy band diagram represents the Fermi level. The thicknesses of the different layers, measured with an atomic force microscope (AFM) are also shown. The active area of the diode is roughly 0.1 cm^2, and measured for each individual device. The production steps of the device are documented in chapter 2.1.2. In this device no final annealing step was made.

2.1.4 P3HT:PCBM bulk-heterojunction device

Here the BHJ SC is introduced. The active film consists of an intermixing P3HT and PCBM bulk, which will be measured with the different techniques.

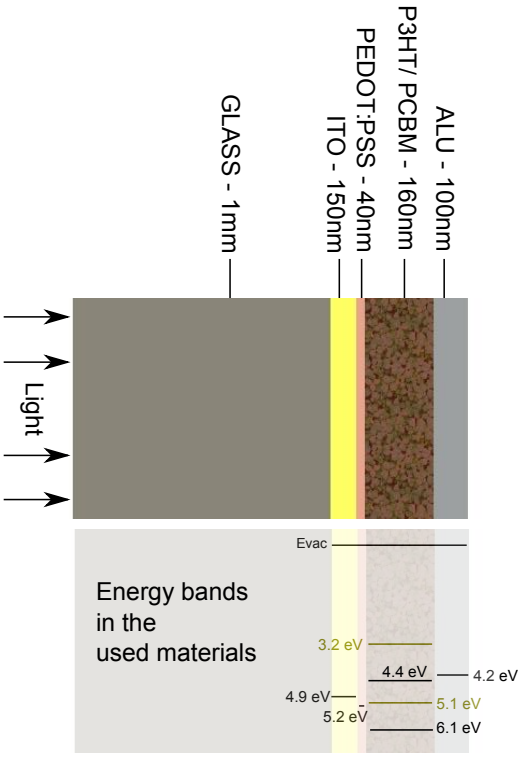

Figure 2.4: Thickness, work functions and electron affinities of an organic solar cell.

In figure 2.4, we see the thicknesses of the films and there work functions respectively electron affinities. The active area is 0.11 cm^2 and has a thickness of 160 nm. The concept of the BHJ solar cell is introduced in chapter 1.2.1. This device was spin coated outside the glovebox.

2.1.5 P3HT device for conductivity measurements

To measure the conductivity in low conductive materials, like P3HT, a new technique is introduced in this section. The device is designed to, not only measure the conductivity, but also the mobility and charge carrier concentration at equal temperature and degradation conditions. With equation $\sigma = en\mu$ the relation between conductivity(σ), mobility(μ) and charge carrier concentration(n) is defined. Each parameter will be measured by itself and should complement each other. In this chapter the device is introduced to measure the mobility by CELIV, the charge carrier concentration by impedance and the conductivity by a modified 4 wire conductivity measurement. This measurements are done in the cryostat (figure 2.11), in order to control the temperature accurately and to prevent any doping by oxygen, since the cryostat works in vacuum.

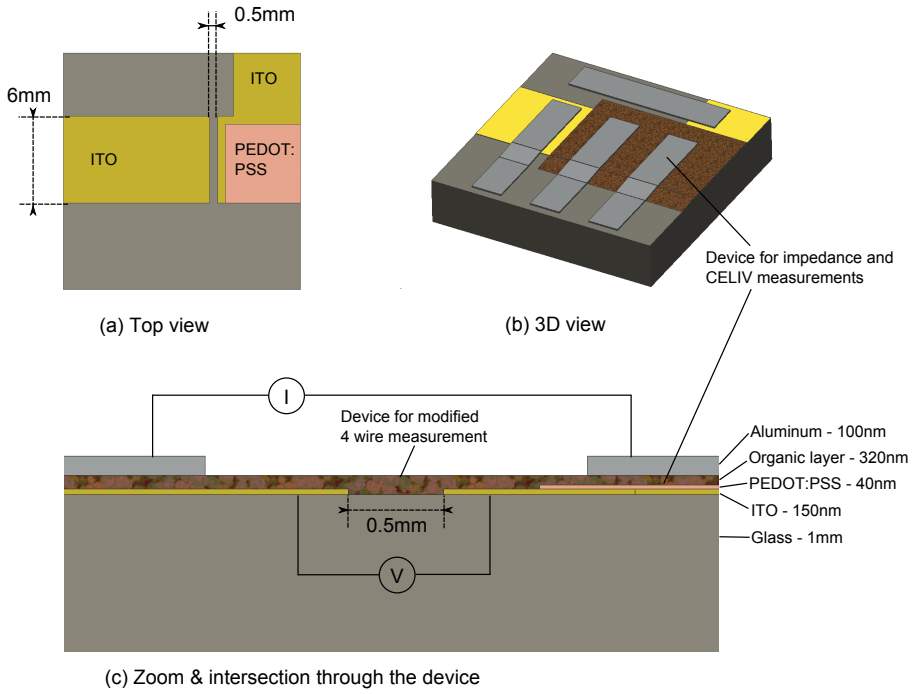

Figure 2.5: Device assembly for impedance, CELIV and modified 4 wire conductivity measurements. (a) Device without organic film and without electrodes. (b) Final device with a diode and a resistance for the modified 4 wire conductivity measurement. (c) Intersection of layers for modified 4 wire conductivity measurement and the connection diagram

To measure mobility, charge carrier concentration and conductivity a device with a special ITO shape is used. In figure 2.5(a) the ITO and the PEDOT:PSS on the glass substrate is shown. The gap of 0.5 mm is used to measure the voltage drop over the organic layer with a modified 4 wire measurement technique. The device for impedance and CELIV measurements is an organic diode between the aluminum and ITO layer. In picture 2.5(c) the connection diagram for the modified 4 wire conductivity measurement by a zoom of the intersection is shown, where the current is sourced on the top aluminum contacts and the voltage is measured at the ITO contacts. The conductivity of the ITO contacts are much higher than from the measured P3HT. Thus, the voltage drop from the measured material in the gap of 0.5 mm is measured. With the intersection area ($A = filmthickness \cdot gapwidth(6mm)$), the length ($l = 0.5\ mm$) of the gap and the measured resistance ($R = V/I$) over the gap, the conductivity can be measured by equation 2.1.

$$\sigma = \frac{l}{R \cdot A} \tag{2.1}$$

For example, with a measured resistance of 1 $G\Omega$ and a film thickness of 200 nm the conductivity would be $4.16 \cdot 10^{-6} \Omega^{-1} cm^{-1}$.
A contact resistance between the ITO and the measured material, for example P3HT, is not considered. Since P3HT and ITO makes a quasi ohmic contact and the measured resistance is in the Giga ohm regime, the contact resistance between ITO and the measured material should not affect the measured resistance significantly.

Mobility, charge carrier concentration and conductivity are geometry independent values, thus

the geometry has to be measured, in order to get a material dependent value for the conductivity. The design from the device is introduced in figure 2.5. The active area of the diode and the real geometry of the resistance have numbered points in figure 2.6. This points are used to calculate the resistance and the active diode area.

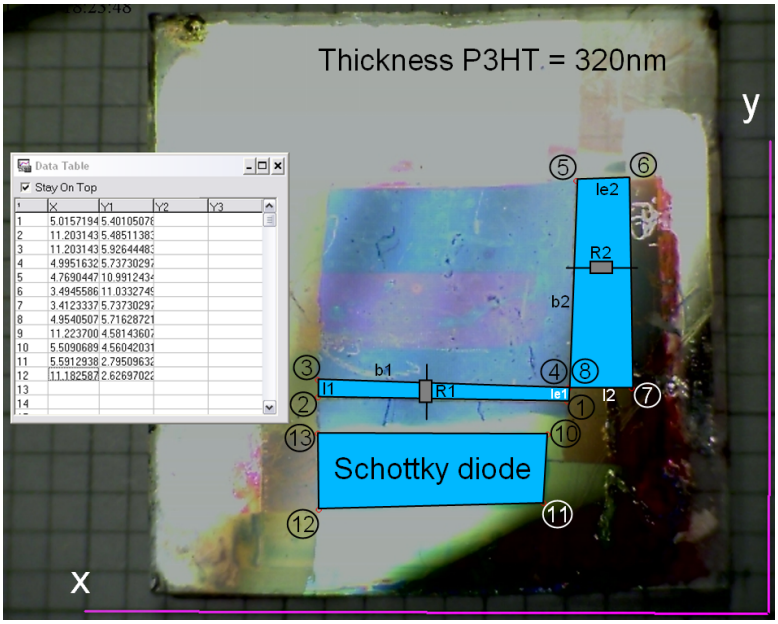

Figure 2.6: P3HT device to measure resistor areas and Schottky diode area. Picture was made with reflecting light, to make the ITO visible. b_1, l_1, l_{e1}, $R1$, b_2, l_2, l_{e2}, $R2$ are the specific lengths.

$$\frac{1}{\sigma R} = th \cdot \int_0^b \frac{1}{l + \frac{(l-l_e)x}{b}} dx = \frac{th}{l} \left(\frac{-b}{1 - l_e/l} \right) \cdot ln \left| \frac{l_e}{l} \right| \tag{2.2}$$

The resistance R1 and R2 have not a rectangular shape, thus the geometry has to be integrated, shown in equation 2.2, to get the conductivity. $1/\sigma R$ is a geometry dependent ratio which gives the inverse conductivity by multiplying with the real resistance of the the device.

Using equation 2.2, which is based on 2.1, the values from figure 2.6 and the thickness measured by AFM $th = 320\ nm$ give:

4 wire resistor R1: $th = 320\ nm$, $l1 = 0.44\ mm$ (P2,P3), $l_{e1} = 0.34\ mm$ (P1,P4),
$b1 = 6.2\ mm$ (P3,P4)
$\rightarrow \sigma \cdot R1 = 1.95 \cdot 10^5 m^{-1}$.

4 wire resistor R2: $th = 320nm$, $l2 = 1.5\ mm$ (P7,P8), $l_{e2} = 1.3\ mm$ (P5,P6),
$b2 = 5.3\ mm$ (P4,P5)
$\rightarrow \sigma \cdot R2 = 8.3 \cdot 10^5 m^{-1}$.

$\sigma R = \sigma \frac{R1 \cdot R2}{R1 + R2} = 1.6 \cdot 10^5 m^{-1}$

With the factor σR, measuring the resistance R gives thus the conductivity of the material. The area of the Schottky diode is defined by points 10-13 (figure 2.6) and is $= 0.1\ cm^2$.

2.1.6 P3HT:PCBM bulk-heterojunction device for conductivity measurements

The layout of the solar cell device is almost the same as the layout used in the P3HT device in last chapter. In this device no parallel resistors are needed to calculate the conductivity by 4 wire technique, because the bulk does is not touch the horizontal electrode and therefore not significantly contribute to the measured resistance.

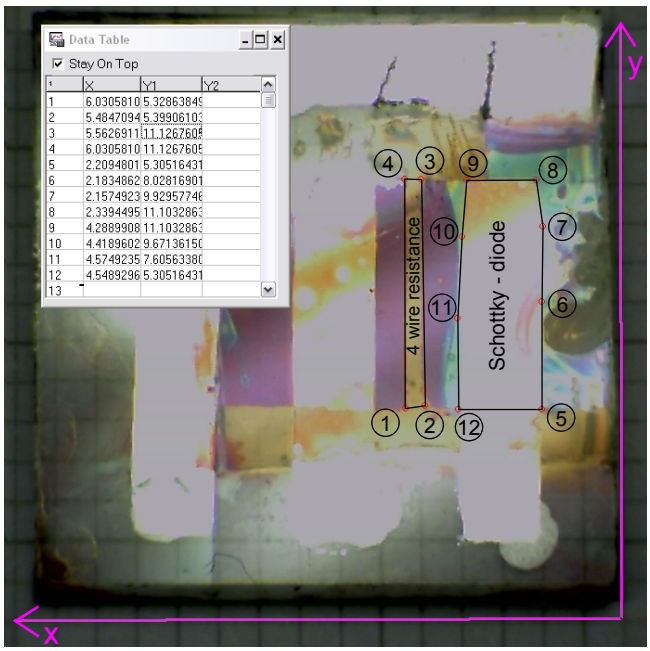

Figure 2.7: Picture of solar cell device. The picture was taken with reflecting light, to make the ITO layer visible. The active area of the Schottky-diode and the 4 wire resistor are shown with there coordinates in x and y axis.

Using equation 2.2, the values from figure 2.7 and the thickness measured by AFM $th = 220\ nm$ give:

4 wire resistor: $th = 220\,nm, l = 0.55\,mm(P1, P2), l_e = 0.47\,mm(P3, P4), b1 = 5.7\,mm(P2, P3) \rightarrow \sigma \cdot R = 4.03 \cdot 10^5 m^{-1}$.

The area of the Schottky diode is defined by points 5-12 (figure 2.7) and is $= 0.13\ cm^2$.

2.2 Equipment

In this chapter the used equipment is introduced. Chambers are needed to prevent variations in the measured quantities due to oxygen exposure. Either the chamber can be filled with nitrogen or argon (small chamber), or the chamber has to be evacuated (cryostat).

2.2.1 Small chamber

The small chamber (figure 2.8) has 2 nitrogen connections. One for the cooling system and one to flood the system. By flooding the system, unwanted gases in the chamber will be removed. During use, a small overpressure keeps the system clean. All electrical connection are BNC connectors and the internal resistances of the wires are very low. Thus, this chamber is the choice for impedance spectroscopy, where frequencies up to 1 MHz are applied to the device.

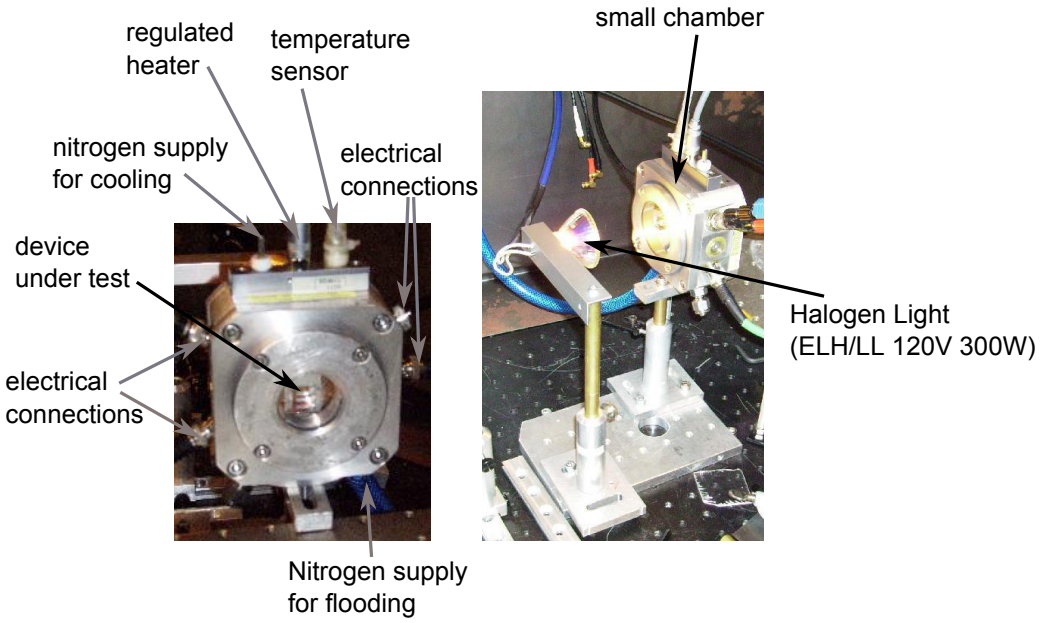

Figure 2.8: Small chamber with device under test and the connections

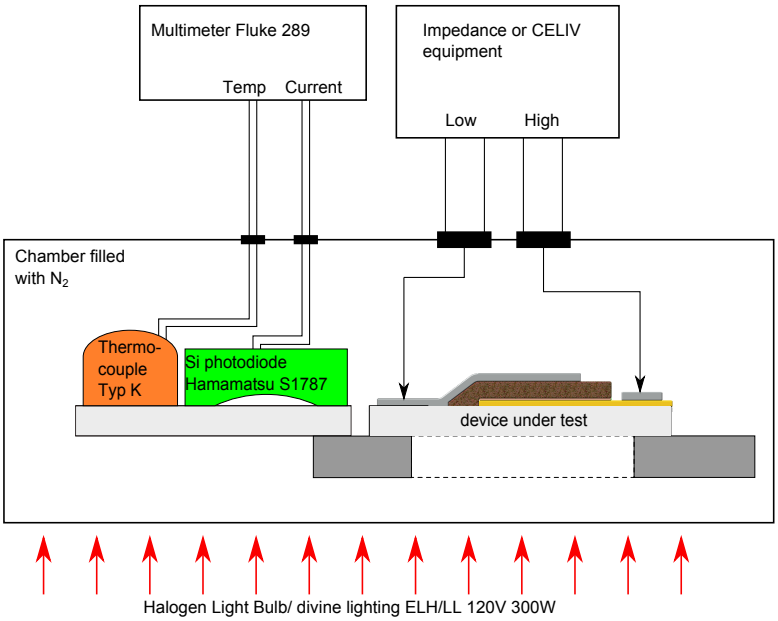

Figure 2.9: Intersection diagram of small chamber. The temperature regulation system is not included

In the small chamber the device lies on a metal holder and is connected to tin wires by silver paste. The temperature is controlled in situ by a thermocouple on to glass surface. The measurement setup has a halogen light bulb, that imitates the spectrum of the sun. The light intensity is adjusted by a transformer. The irradiance is controlled with a silicon photo diode (see figure 2.9) by measuring the short circuit current, which is proportional to the light intensity. The system was calibrated to an intensity of 100 mW/cm^2 (irradiance of AM1.5). In the measurements the light intensity on the device was changed from dark to 100 mW/cm^2. The difference in the spectrum, due to different temperatures of the halogen bulb is recorded and showed in figure 2.10. The peaks of the curves do not change significantly by decreasing irradiance with respect to the spectrum, thus the device is excited from about the same energies (wavelength) during the exposure of lower intensities.

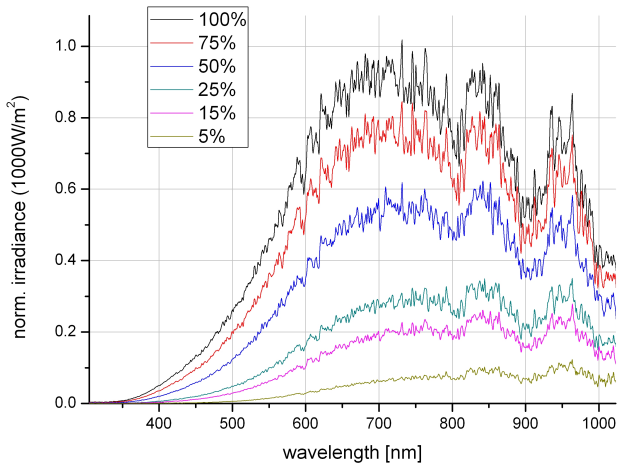

Figure 2.10: Spectrum of halogen light bulb (ELH/LL 120 V, 300 W) at different intensities

2.2.2 Cryostat

The Cryostat was used to make accurate temperature measurement between 200 K and 300 K. The cooling of the cryostat is done by liquid nitrogen. The nitrogen flux through the cryostat can be manually adjusted with a valve. To regulate the cryostat on a constant temperature, a heater is integrated. The heater is controlled automatically by an external unit with a PID regulation. During the measurements the device is in vacuum and thus is not exposed to air. The disadvantage of the cryostat is the internal resistance. The cables from the cryostat have a resistance of 30 Ω, therefore it is not the appropriate choose to make measurements at higher frequencies. But for low frequencies (20-500 Hz) impedance will not be significantly affected by this series resistance.

There is also a window to illuminate the sample. To avoid a heating of the device, the measurements with the cryostat are done with a light intensity of 5 mW/cm^2 (5 % irradiance of AM1.5). In this setup the lamp was running with full power, where the spectrum is most similar with AM1.5, but the distance of the lamp was increased. The mismatch of the spectrum from the lamp compared to AM1.5 is shown in figure 2.12.

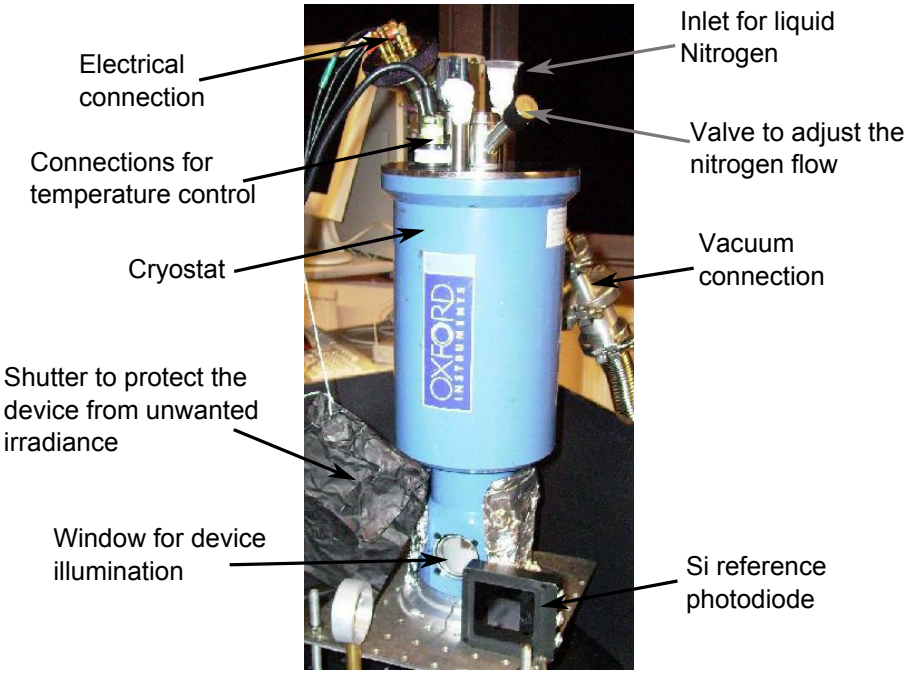

Figure 2.11: Cryostat and his connections

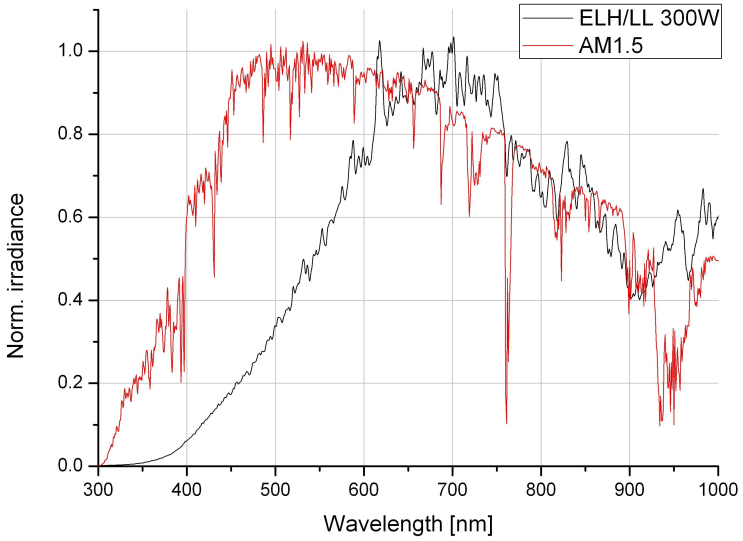

Figure 2.12: Spectrum of halogen lamp ELH 120V and from AM1.5

2.2.3 Apparatus

The vacuum pump is connected to the cryostat and it achieves a vacuum of about $4 \cdot 10^{-5}$ mbar. The cryostat is not directly visible in figure 2.13. The device in the cryostat is illuminated from the Halogen light bulb. The distance from the light source to the device in figure 2.13 is

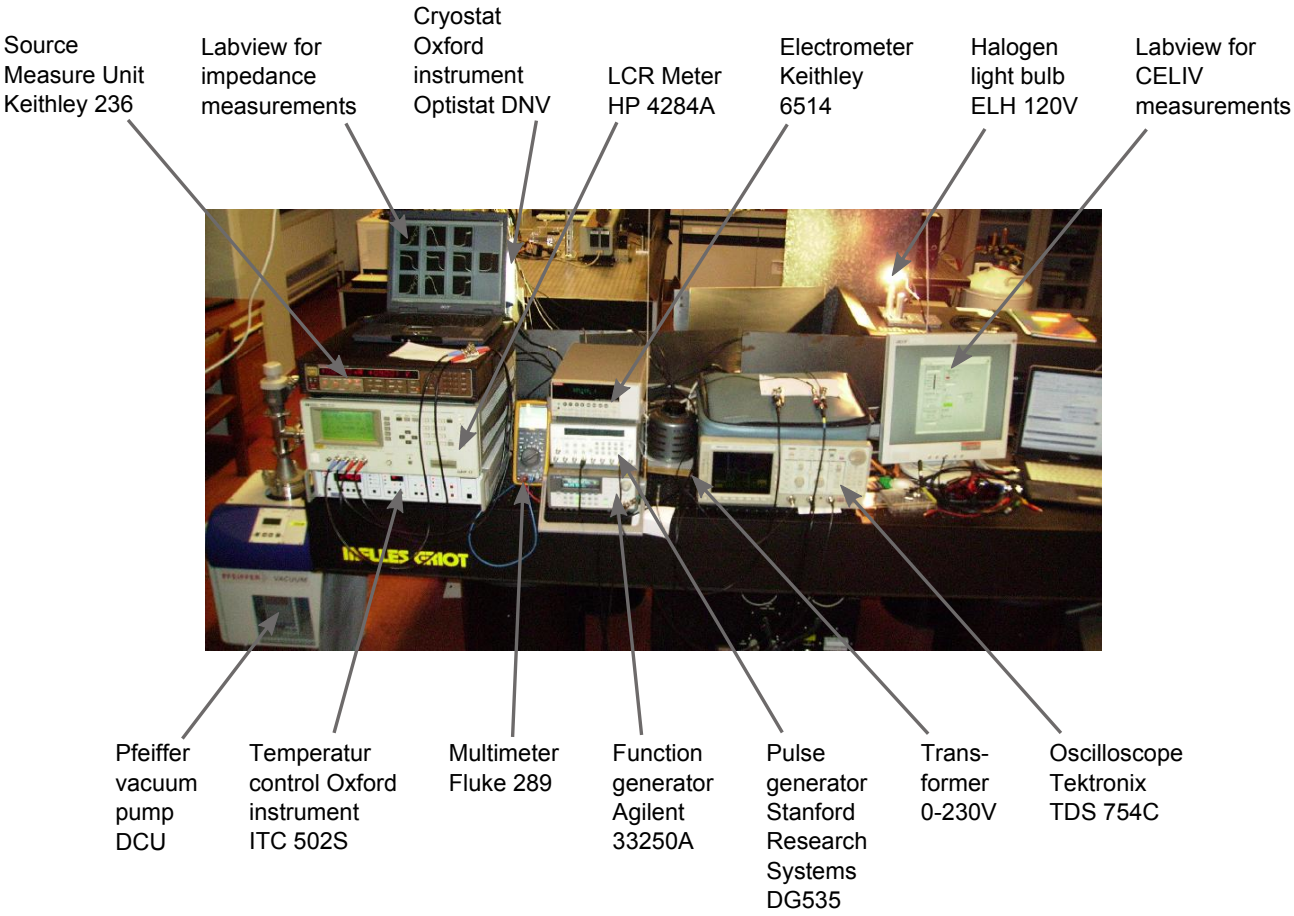

Figure 2.13: Test equipment for impedance, CELIV and 4 wire conductivity measurements

adjusted to have 5 mW/cm^2 intensity on the device, this is controlled by a reference silicon diode. The temperature control unit regulates the current from the heater in the cryostat, and reads the information from the temperature sensor in the cryostat to regulate a user defined temperature. For impedance measurements the LCR meter is used. The LCR meter works in 4 wire mode and is directly connected to the cryostat. An external LabView program can be used to define a measurement procedure. The program was defined to make measurements between 20 Hz and 1 MHz and between -2 V and +2 V.

The CELIV setup is connected like in figure 1.6. The function generator, which is triggered by the pulse generator, applies a positive ramp on the negative connection from the device (aluminum electrode). The positive connection of the device (ITO electrode) is connected to the oscilloscope. The internal resistance of 50 Ω works as a shunt. Thus, the oscilloscope shows a voltage which is proportional to the current through the device. Both, the function generator and the oscilloscope are grounded, this is where to current flows back to the function generator. Additionally there is a laser system (Continuum Surelite OPO Plus 355 nm). The laser is pointing on the device. The pulse generator controls the timing to the laser and to the function generator. All pieces of equipment are connected over GPIB to the LabView software, from where all necessary parameters can be adjusted.

For the modified 4 wire conductivity measurements, the current is sourced by the Keithley 236 (see figure 2.13). To use the Keithley 236 was necessary, because of sourcing in the nano ampere range, since the film resistance is in the giga ohm range. To measure the voltage drop, a Voltage meter with a very high internal resistance is needed. An electrometer like the Keithley 6514 with an almost infinite resistance was used.

The Keithley 236 was also used to measure the IV characteristics of the device, here one applies different voltages on the device and measures the current response.

Chapter 3

Behavior of pure P3HT films

In this chapter a pure P3HT film (see 2.1.1.1) will be investigated with different measurement techniques.

3.1 IV behavior of P3HT films

In this section IV measurements with the Schottky device, introduced in section 2.1.3, measured in the small chamber (2.2.1) are shown.
In according to Campbell [16], the Trap-Free-Space-Charge-Limited-Current (TFSCLC) theory in organic materials can be used, if the hole injection electrode ITO is treated by either a plasma or by a PEDOT:PSS layer, as in this device. Organic diodes show an ohmic behavior at a low positive voltage, and a SCLC behavior at higher positive voltage. Here we use the Mott-Gurney law (equation 1.1), where the temperature and E-field dependence of the mobility is not taken into account.

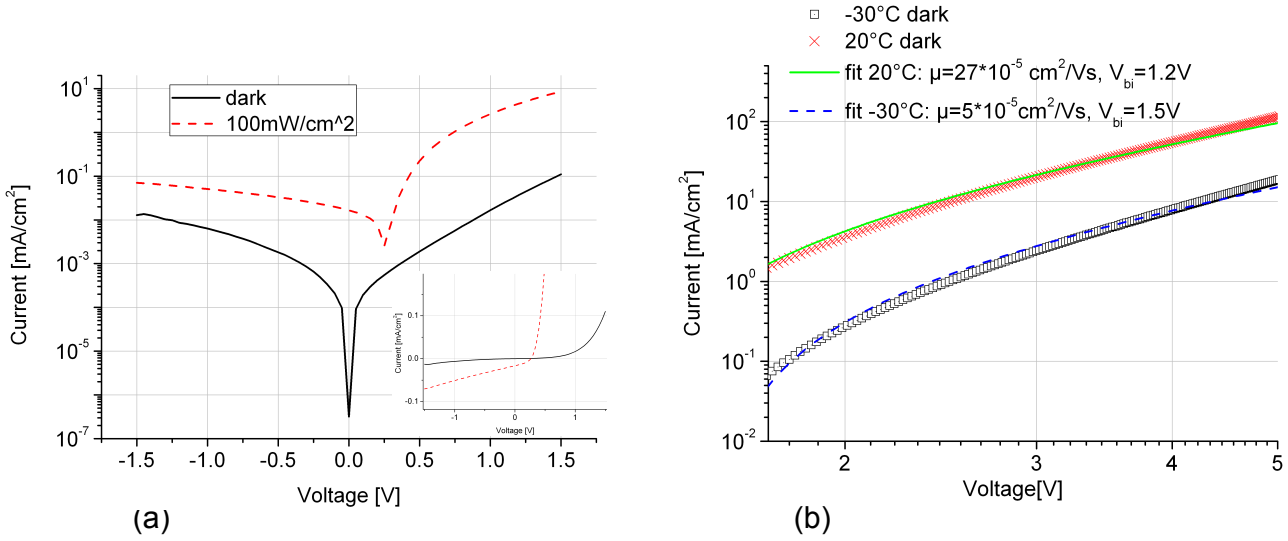

Figure 3.1: IV measurements of the pure P3HT device. (a) IV in log scale (inset in linear scale). (b) IV curve with corresponding SCLC model fit.

The IV curves (3.1(a)) show a lower current in the dark. A small open circuit voltage of about 0.25 V at a light intensity of 100 mW/cm^2 (equal to AM1.5) is also recognizable. Thus the pure P3HT device works as a solar cell under illumination. The measured IV characteristics and the corresponding fits to the SCLC model are shown in figure 3.1(b). At 20 $°C$ a built-in potential of 1.2 V and a mobility of $27{\cdot}10^{-5}$ cm^2/Vs is calculated. At -30 $°C$ the built-in potential increases to 1.5 V, whereas the mobility decreases to 5 $\cdot 10^{-5} cm^2/Vs$. The mobility is lower at -30 $°C$, since the mobility in organic devices depend on the hopping process, which is temperature dependent [17].

3.2 Mobility in P3HT films

The CELIV technique was used to investigate how the mobility in the P3HT device depends on the temperature, the continuous white-light illumination and on different bias voltages. For all the measurements in this chapter, the mobility was calculated with equation 1.9. A laser pulse of 355 nm was used to create additional charge carriers on top of the white light, for the Photo-CELIV measurements.

3.2.1 Mobility dependence on temperature

In this subsection mobility is measured with the P3HT device, introduced in section 2.1.5. The device is measured in the cryostat (2.2.2) and the mobilities in figure 3.2(a) will be used to calculate to conductivity in section 3.4.

Transients measured without laser and in the dark do not show any bump, indicating low extracted charge carriers, thus they are not shown here.

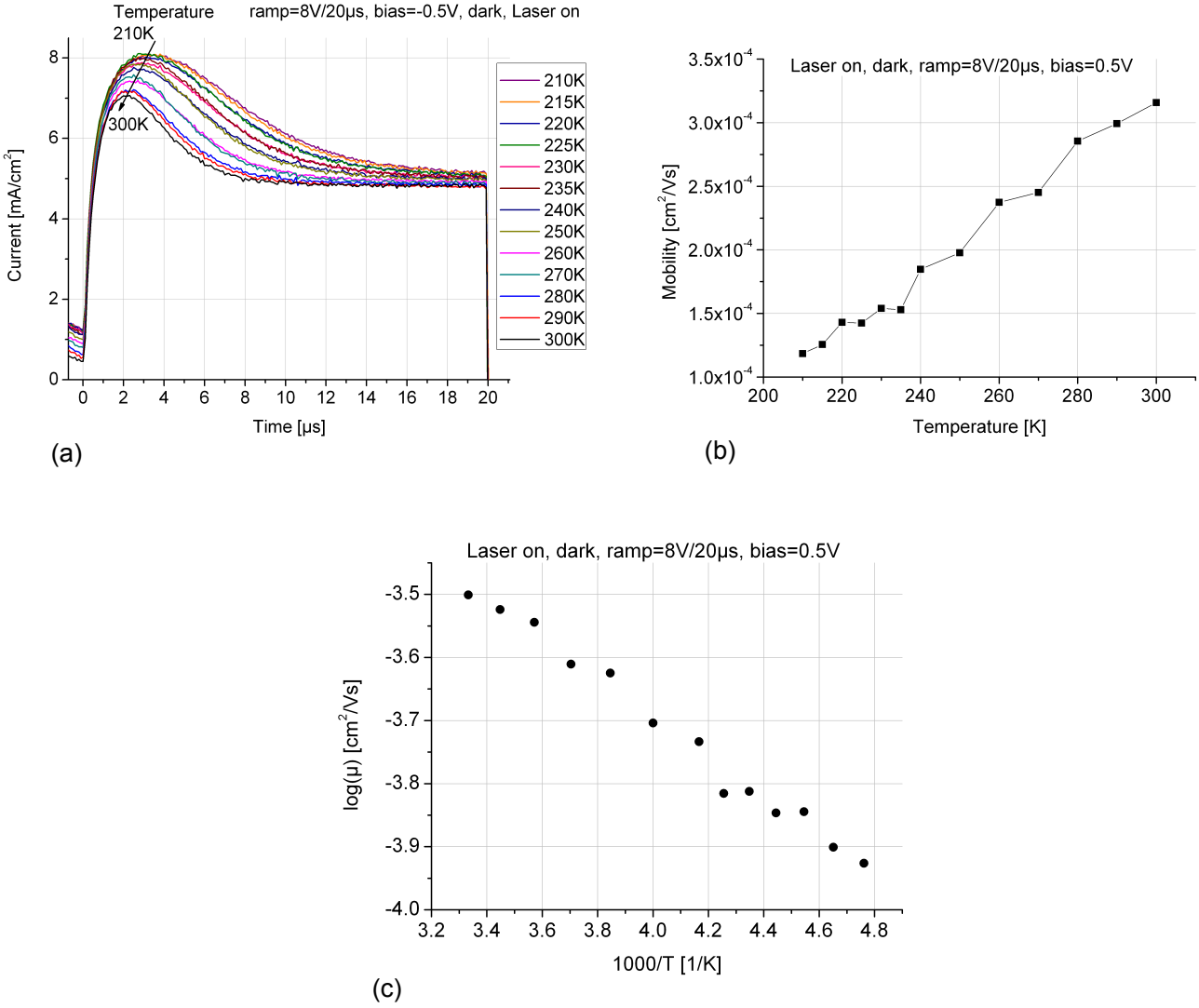

Figure 3.2: CELIV measurements on pure P3HT device at different temperatures. (a) CELIV transients. (b) Calculated mobility by equation 1.9. (c) Arrhenius plot of the mobility

For figure 3.2(b) the mobilities of 3.2(a) are calculated. The mobilities have a linear behavior by increasing temperature. In the Arrhenius plot in figure 3.2(c) the mobility also seems to be linear. From this resolution it is not possible to find out, if the Arrhenius plot or the linear plot of the mobility has a linear behavior.

3.2.2 Mobility dependence on illumination intensity

In this subsection mobility measurements with the Schottky device, introduced in section 2.1.3, measured in the small chamber (2.2.1) are investigated.

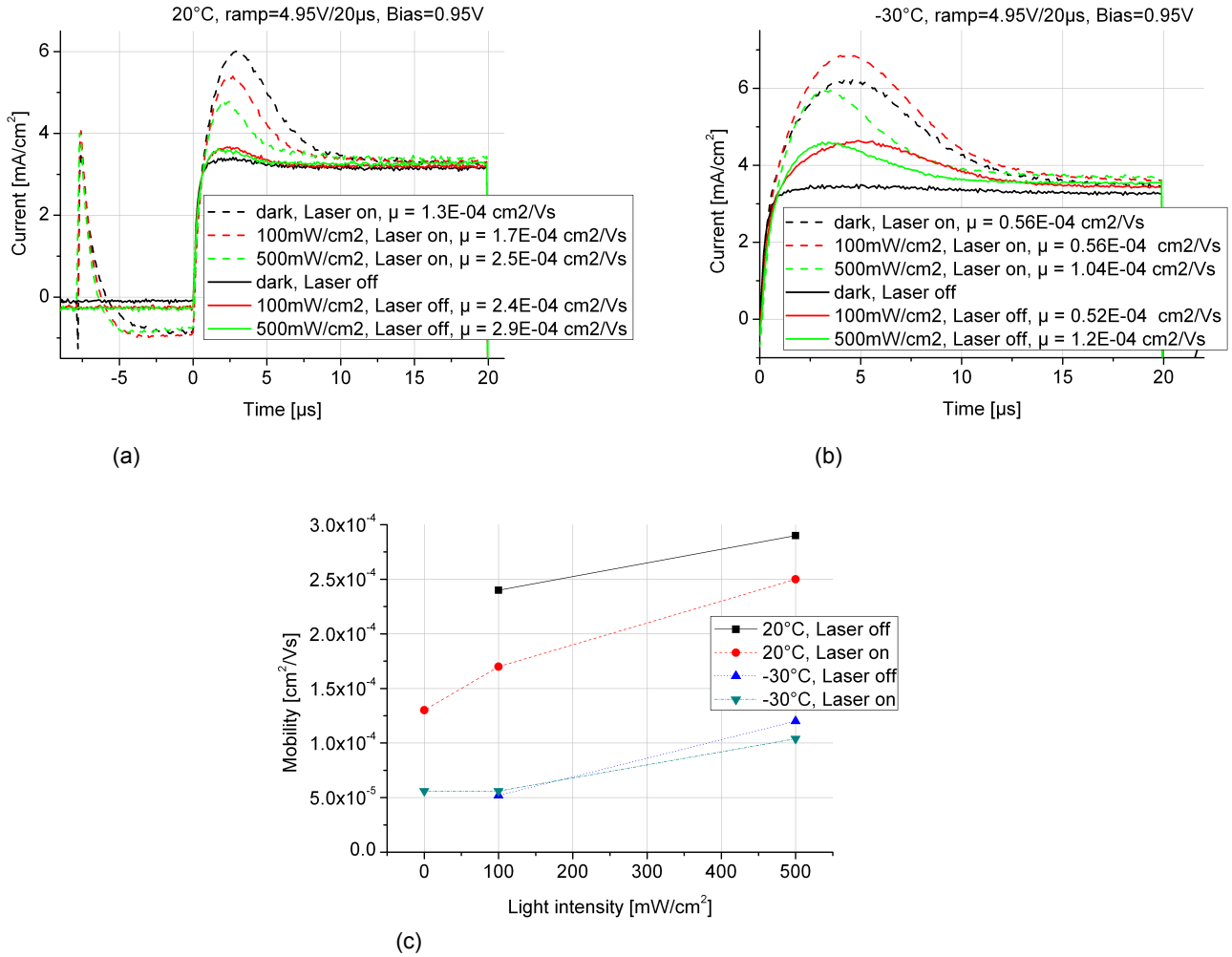

Figure 3.3: CELIV measurements on a P3HT device. (a) Mobility dependence on light at 20 $°C$. (b) Mobility dependence on light at -30 $°C$. (c) Mobility overview at different temperatures and with/without laser

Classical CELIV curves are shown in figure 3.3(a). At -8 μs the laser is flashing. Positive and negative charges are created over the whole film. Without a special device construction it is not possible to distinguish between the extraction of holes and electrons. But if the device is thick enough, photo generated charges are not anymore in the bulk, but at the surface, which makes it possible to differ between holes and electrons. The bulk of the device has a thickness of 230nm and thus the assumption of uniformly photo generated charges in the bulk is a good approximation. Therefore, we can not distinguish between hole and electron mobility, but it is generally accepted that the holes in pure P3HT film mainly contribute to the charge transport [3]. An external DC bias is applied to minimize the electric field in the film prior to the extraction pulse. At 0 μs the ramp starts. Due to the increasing voltage the depletion layer

gets bigger and the holes are extracted by the ITO electrode. After equation 1.9, the time of the extraction peak gives the mobility.

The specific mobilities are shown calculated in the legend of figure 3.3(a) and 3.3(b) or in the overview 3.3(c). One can recognize, the higher the illumination the higher the mobility. But, the local temperature of the film may increase upon illumination, and the higher the temperature, the higher the mobility. Even when we measure the surface temperature with a thermocouple, it is difficult to know, whether the mobility increase comes from higher illumination or higher temperature of the film. With a laser pulse the mobility gets lower compared to the transients without laser pulse.
The charge carrier concentration (area below the bump) gets lower with higher light intensity. This is contrary to the expectations, since at least the same amount of charges should be photo generated at higher light intensities. This phenomenon requires more investigation.

In figure 3.3(b) at -30 $°C$ the mobility dependence looks similar. Increasing the light intensity induces higher mobility, although the mobility at 100 mW/cm^2 (light intensity of one sun) is equal to the mobility in the dark. Without accurately knowing film temperature it is difficult to make any conclusion with high illuminated films. But we can see in this graph a agreement of the mobility with and without laser. The mobility at 1 sun with a laser pulse is $0.56 \cdot 10^{-4}$ cm^2/Vs compared to $0.52 \cdot 10^{-4}$ cm^2/Vs without laser pulse. And also the mobility in the dark with $0.56 \cdot 10^{-4} cm^2/Vs$ is similar. At -30 $°C$ the mobility is not dependent on the laser pulse and at 20$°C$ the mobility is dependent on the laser pulse.

The current at 20 μs at 100 mW/cm^2 and 20 $°C$ is 3.3 mA/cm^2 and with a capacitor area of $A = 0.105$ cm^2 the real current is 0.33 mA. This current can be used in equation $C = i\frac{dt}{dU} = i/ramp = 0.33mA/(4.95V/20\mu s) = 1.33nF$, which is the geometric capacitance of the diode. The thickness of the capacitor can be calculated by $d = \varepsilon\varepsilon_0 A/C = 209$ nm with $\varepsilon = 3$. This is in a good agreement with the thickness of the film measured by AFM (230 nm).

To summarize, the mobility in P3HT increases towards higher temperatures. Mobility depends on different permanent light intensities, probably due to the increasing temperature of the film. At 20 $°C$ the mobility gets lower with a laser pulse, whereas at -30 $°C$ the laser pulse does not affect the mobility significantly.

3.2.3 Mobility dependence on bias voltage

In this subsection the mobility of the holes in the P3HT film, introduced in section 2.1.3, dependent on the applied bias and on the slope from the applied ramp will be measured and discussed. The device was measured in the small chamber (2.2.1).

CELIV transients with different bias voltages of 0 V and 0.95 V are shown in figure 3.4(a) and 3.4(b). In picture 3.4(c) at a bias of 1.3 V, the diode is in forward bias, and we inject many charge carriers into the film, which are visible in the negative current before the pulse begins.

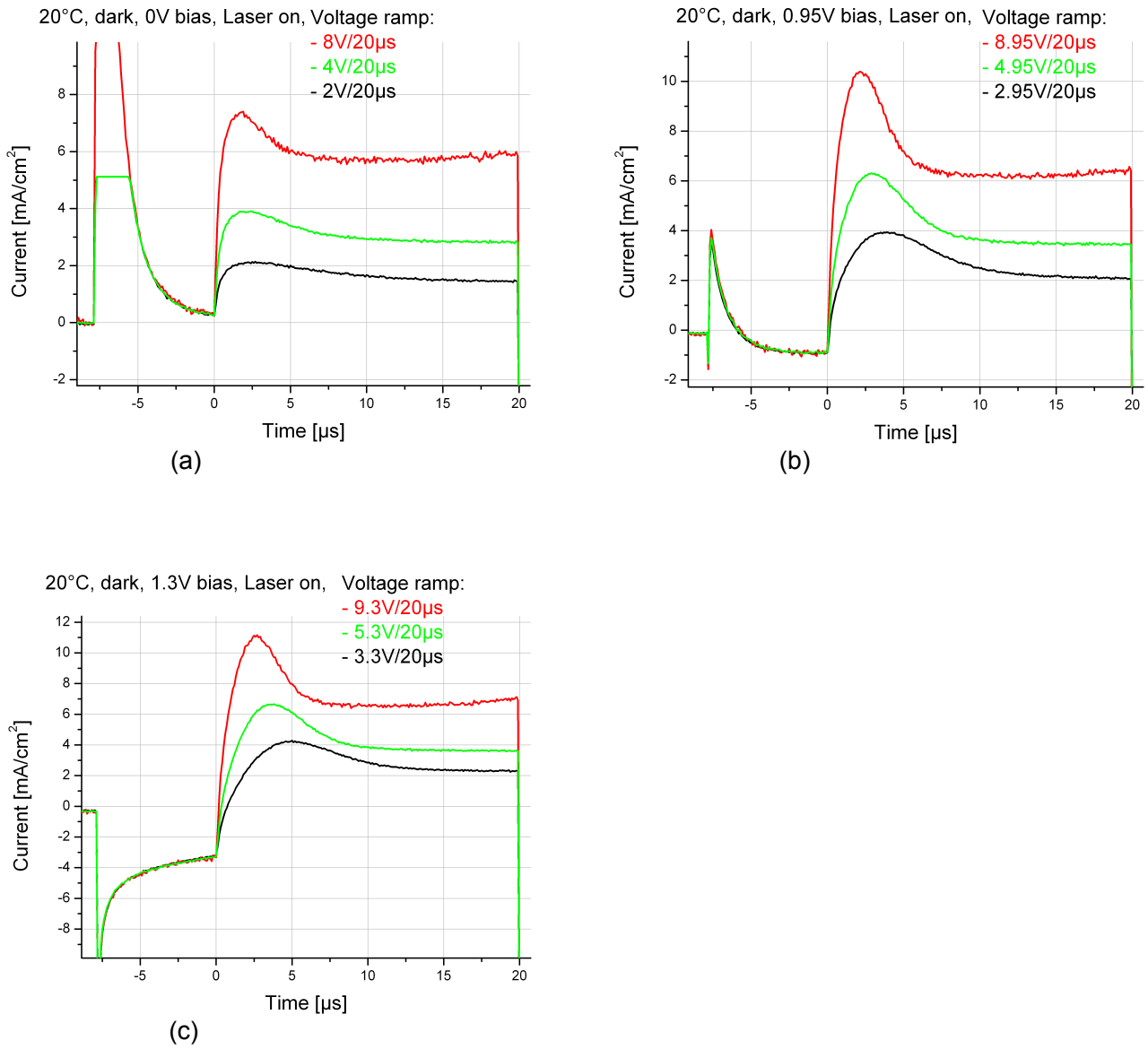

Figure 3.4: Photo-CELIV measurements on a P3HT device at 20 $°C$ with different ramps and with: (a) Bias voltage = 0 V, (b) Bias voltage = 0.95 V, (c) Bias voltage = 1.3 V

Mobilities	$Bias = 0V$	$Bias = 0.95V$	$Bias = 1.3V$
High slope	$2.7 \cdot 10^{-4} cm^2/Vs$	$1.3 \cdot 10^{-4} cm^2/Vs$	$0.88 \cdot 10^{-4} cm^2/Vs$
Middle slope	$3.9 \cdot 10^{-4} cm^2/Vs$	$1.3 \cdot 10^{-4} cm^2/Vs$	$0.76 \cdot 10^{-4} cm^2/Vs$
Low slope	$4.7 \cdot 10^{-4} cm^2/Vs$	$1.2 \cdot 10^{-4} cm^2/Vs$	$0.63 \cdot 10^{-4} cm^2/Vs$

Table 3.1: Mobility dependence on bias voltage and on the slope of the voltage ramp

The mobility (table 3.1) seems to be dependent on the applied slope from the ramp and on the bias voltage. The higher the bias, the lower the mobility. This may be because a higher bias voltage induces a smaller depletion layer (see in figure 3.9). And with a smaller depletion layer one extracts more charges and it also takes more time (t_{max}) to extract them, because the mobile charges are distributed over a broader area in the film. The mobility calculations

(equation 1.9) do not consider a depletion layer, one assumption is a uniform distribution of mobile charges in the film.

At a bias of 0V the mobility decreases with a higher slope of the ramp (table 3.1). At a bias of 1.3 V the mobility increases with a higher slope. But the mobility should not depend on the slope of the ramp, since we consider the ramp in equation 1.9. At a bias of 0.95 V the mobility is almost independent on the slope of the voltage ramp. By measuring CELIV it is common sense, to adjust the bias voltage to a value where the extracted charges before the ramp are minimized. This is how the bias voltage 0.95 V was defined in this CELIV measurements.

By using a bias voltage, which minimizes the extracted charges before the voltage ramp, the mobility does not depend on the slope of the ramp.

3.3 Charge carrier concentration in P3HT films

3.3.1 Charge carrier concentration dependence on bias voltage

For this measurements the P3HT device (introduced here: 2.1.3) was used, which was measured in the the small chamber (2.2.1).

Since it is possible to measure not only the mobility, but the charge carrier concentration by the CELIV technique, it is the interest now to measure the charge carrier concentration at different bias voltages. The obtained CELIV curves are shown in figure 3.5(a). The area under the curve reflects to the charge carrier concentration. The charge carrier concentration seems to have an exponential dependence on the voltage, see figure 3.5(b) in log scale. The assumption of an exponential behavior implies a correlation to the exponential IV curve from a diode.

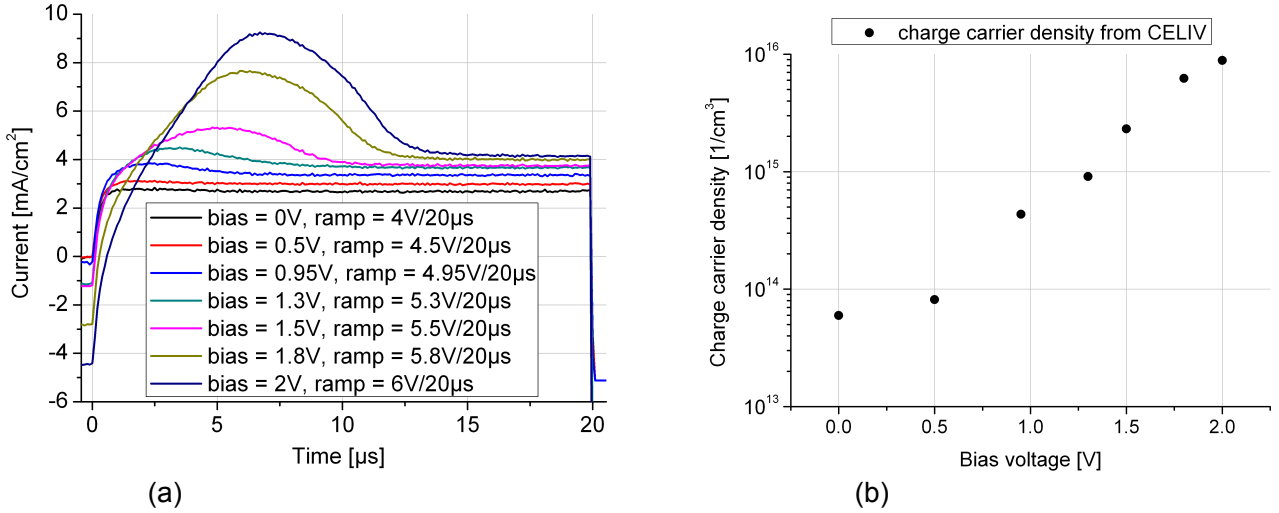

Figure 3.5: Measuring charge carrier concentration by CELIV at 20 $°C$, with a light intensity of 100 mW/cm^2 and without a laser pulse. (a) CELIV Signal at different bias levels, where the area under the bump refers to the charge carrier concentration. (b) Measured charge carrier concentration dependent on the bias voltage in log scale.

The charge carrier concentration depends exponentially on the bias voltage. This gives rise to the assumption, that with CELIV one measures not only the intrinsic carriers but also the injected carriers. CELIV is not the appropriate technique to measure intrinsic charge carrier concentration in low conductive materials, because with zero bias no visible charges are extracted and with a bias one probably extracts the injected charge carriers.

3.3.2 Charge carrier concentration dependence on temperature

3.3.2.1 Measured by impedance

In this subsection charge carrier concentration is measured with the P3HT device, introduced in section 2.1.5. The device is measured in the cryostat (2.2.2), and the charge carrier concentrations will be used to calculate to conductivity in section 3.4.

To measure charge carrier concentration on a Schottky-type P3HT device, the well established Mott-Schottky $1/C^2$ plot is used. The lines in figure 3.6(a) are approximations to the points in the slope of the Mott Schottky plot. A slope of a line is inverse proportional to the charge carrier concentration. With equation 1.8, one can calculate the charge carrier concentration. In figure 3.6(a) the Mott-Schottky plot at different temperatures, in the dark and at a light intensity of 5 mW/cm^2 is visible. The charge carrier concentration (figure 3.6(b)) is not temperature dependent, therefore no new charges are generated by increasing thermal excitation. This makes sense by considering the thermal energy at room temperature of 25 meV, which is not enough to lift an electron into the LUMO of P3HT, this would need about 1.9 eV. As soon light hits the sample, the charge carrier concentration doubles. The pure P3HT device should not

act like a photo diode, and charges should not be generated by light, since there is no acceptor in the bulk to separate the excitons. But charges can also be photo generated at impurities or at the junctions to the electrodes (see section 3.3.3), this likely causes the increase of the charge carrier concentration under illumination.

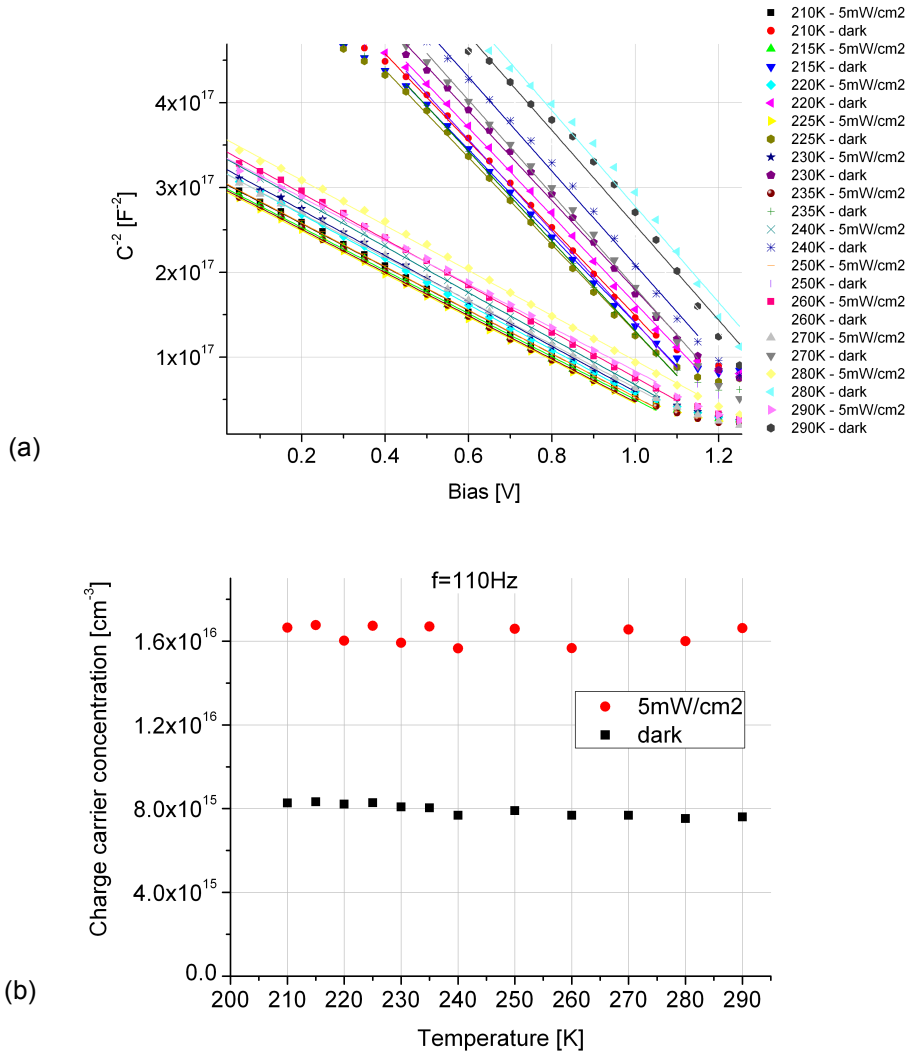

Figure 3.6: Mott-Schottky plot of P3HT device at different temperatures and light intensities (a). Impedance is measured at 110 Hz. From (a) charge carrier concentration is calculated and shown in (b) at different temperatures

The charge carrier concentration in a P3HT device does not depend on the temperature, and doubles with an irradiance of 5 mW/cm^2.

3.3.2.2 Measured by CELIV

In this subsection the carrier concentration is measured with the CELIV technique. The device is introduced in section 2.1.3, and was measured in the small chamber (2.2.1). The charge

carrier concentrations will be used to calculate to conductivity in section 3.4.

The bump below the curve is very small (see figure 3.7(a)), which indicates low amount of extracted charges. Nevertheless, with a illumination of 5 mW/cm^2 one can extract and calculate the charge carrier concentration, which is shown in figure 3.7(b).
The charge carrier concentration decreases with higher temperature and is about 50 times lower than measured with the Mott-Schottky plot, see figure 3.6(b).

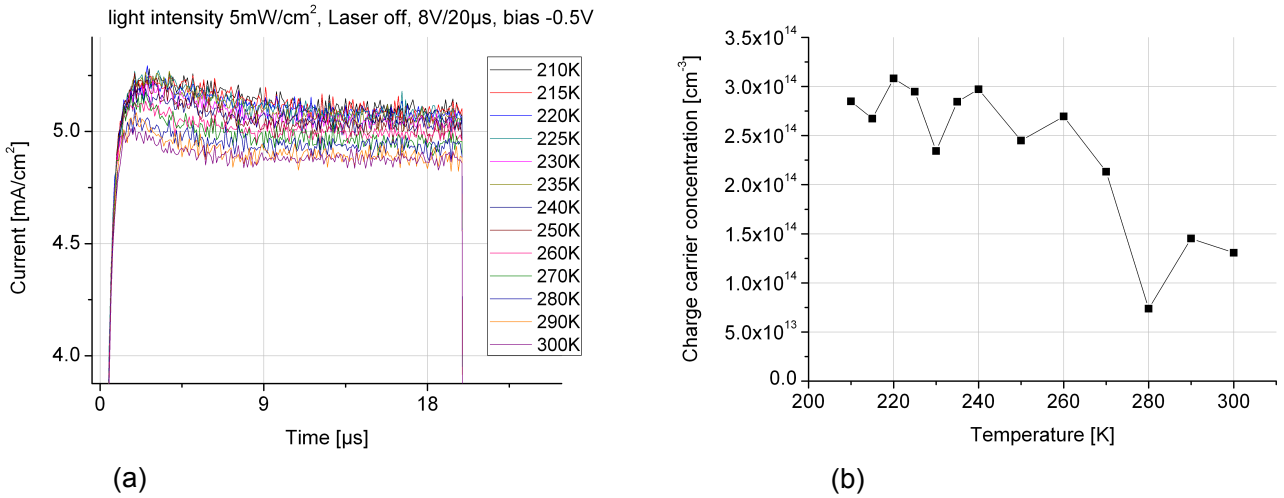

Figure 3.7: (a) CELIV curves at varying temperatures, without Laser pulse and with 5 mW/cm^2 permanent illumination. (b) Measured charge carrier concentration from the CELIV transients

3.3.3 Charge carrier concentration dependence on light

For this measurements the P3HT device (introduced here: 2.1.3) was used, which was measured in the small chamber (2.2.1).

With impedance measurements and equation 1.8 it is possible to measure charge carrier concentration, if the device has a Schottky contact. In order to know how the illumination affects the charge carrier concentration, the film was illuminated in situ. Figure 3.8 shows the Mott-Schottky behavior at 20 °C, -30 °C and different light intensities. The slopes of the visible fitting lines are inverse proportional to the charge carrier concentration. The intersection of the fitting lines with the bias voltage axis represents the the built-in potential. The black fitting lines in the dark show a similar charge carrier concentration of $0.77 \cdot 10^{16}$ cm^{-3} at 20 °C and $1.1 \cdot 10^{16}$ cm^{-3} at -30 °C and a built-in potential between 1.1-1.2 V. Once the film is illuminated with 5 mW/cm^2, the charge carrier concentration doubles, but stays at this value by further increasing light intensity. Since we do not have an acceptor, charges should not be generated. But charges can also be photo generated at impurities or at the junctions to the electrodes. By further increasing the light, no additional charges are generated anymore. It seems that a light intensity of 5 mW/cm^2 already saturates the possible amount of photo generated charges. This effect is visible at 20 °C and at -30 °C.
The C^{-2} curve in the dark has an edge at 0.4 V bias voltage. The capacitance at 0.4 V is about

1.5 nF. The capacitance calculated in section 3.2.2 is 1.33 nF. Thus at low voltages in the dark, the measured capacitance is the geometric capacitance.

The built-in potential decreases by increasing irradiance. The black dots in the dark, show a decrease of the built-in potential at higher temperature. Thus, the decrease of the built-in potential with higher illumination could also come from the increasing film temperature induced by high light intensity.

To summarize, the temperature does not have a high influence on the charge carrier concentration. A small light intensity of 5 mW/cm^2 doubles the charge carrier concentration in the film, whereas it stays constant by further increasing the irradiance.

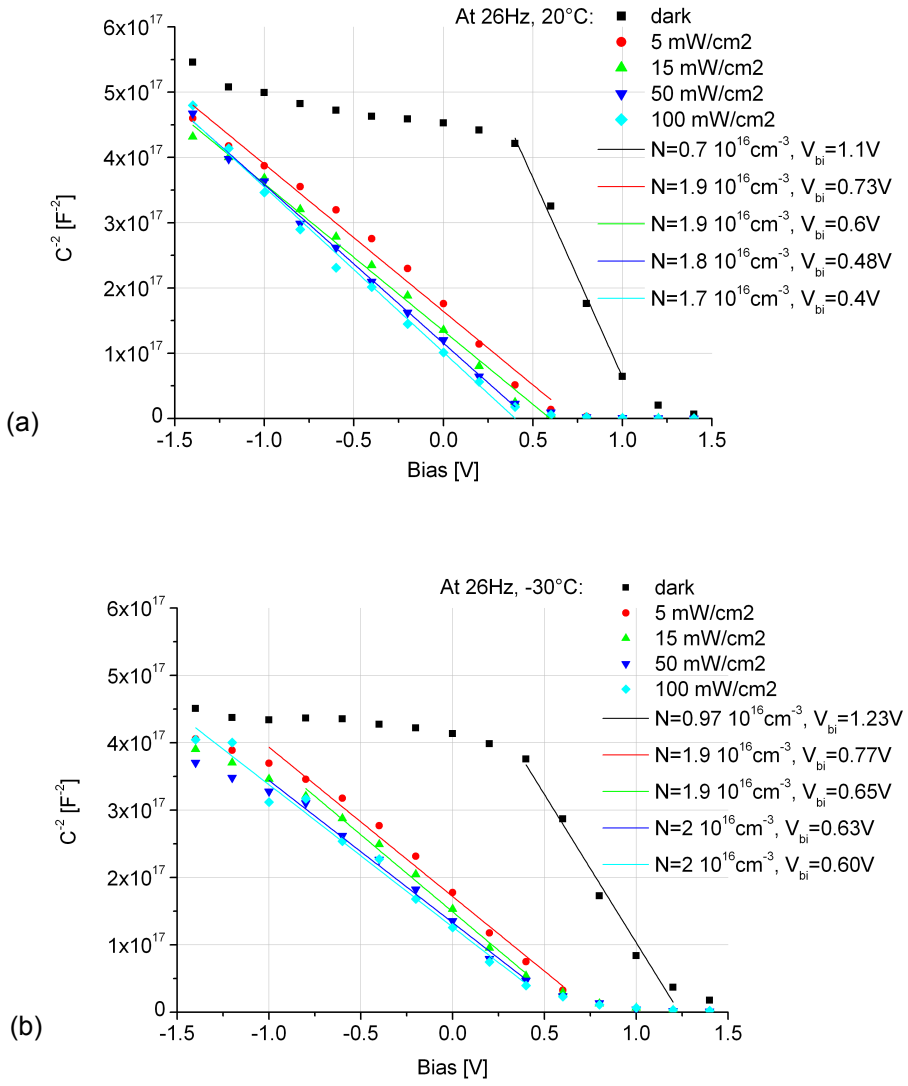

Figure 3.8: Mott-Schottky plot to measure the charge carrier concentration ($N_D \propto slope^{-1}$) and the built-in potential (V_{bi} =intersection with x axis). (a) at 20 °C and 0-100 mW/cm^2 light intensity. (b) at -30 °C and 0-100 mW/cm^2 light intensity

3.3.4 Depletion layer thickness dependencies

With the built-in potential and the charge carrier concentration from last section (3.3.3) one can calculate the depletion layer thickness by using equation 1.5, which is dependent on the bias voltage. This equation is only valid, if the curve in the Mott-Schottky plot is linear. The results and the marked valid regions from this calculations are shown in figure 3.9 at different temperatures and illuminations.

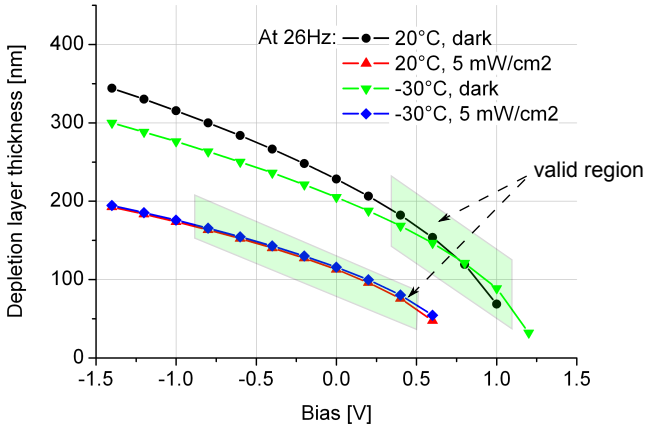

Figure 3.9: Depletion layer thickness of a P3HT device over bias voltage at different temperatures and light intensities. The valid region shows where the Mott-Schottky plot is linear

Measured by AFM the thickness of the film is 230 nm. The depletion layer in a Schottky diode changes its thickness due to different bias voltages, and therefore the capacitance gets lower, the bigger the depletion layer is. Once the depletion layer is thicker than the device, one should not observe any change in the capacitance. In the dark at negative bias in figure 3.9 the depletion layer gets bigger than the thickness of the device, and the capacitance should not change anymore. This, we can observe in figure 3.8. The still visible error may come from an error of the measured active area. Also, the dielectric constant could be different from 3. We already got a smaller thickness of the film in CELIV measurement (209 nm), where we also uses the same dielectric constant. Under light the thickness of the depletion layer is not bigger than the real thickness of 230 nm, in the measured voltage range.

Measured by two completely different methods, AFM and Mott-Schottky plot, the thickness of the film is very similar. The well established theory of Mott-Schottky to define the charge carrier concentration and the depletion layer thickness seems to be accurate in a pure P3HT film.

3.3.5 Impedance spectroscopy

Impedance spectroscopy is a tool to find the equivalent circuit for a device. An equivalent circuit model gives information about the resistance behavior.

The impedance was measured between 20 Hz and 1 MHz, at different bias values and with a AC amplitude of 20 mV rms. In figure 3.10 we see the Nyquist plot of the impedance. A Nyquist plot shows the impedance in a diagram with complex axis, where the abscissa is the real and the ordinate the imaginary axis. The black dots in both figures are the measured points at a bias of 1 V, 20 $°C$ and in the dark. We observe a behavior from a capacitor with a parallel and a series resistance, see figure 3.11.

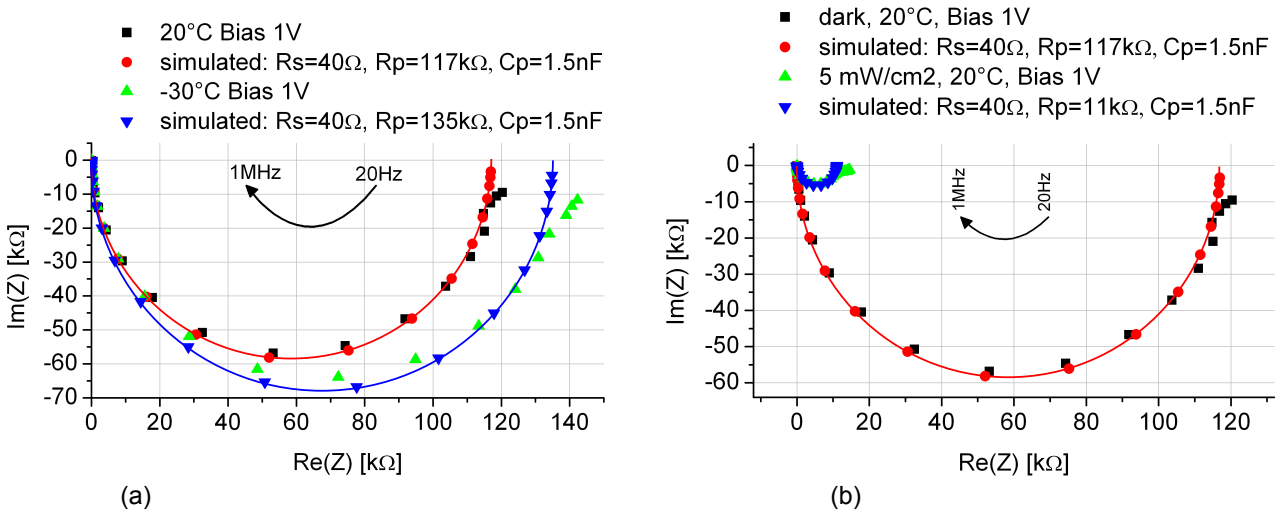

Figure 3.10: Impedance spectroscopy on the P3HT device at 1 V bias with simulated equivalent circuit curve. (a) at 20 $°C$ and at -30 $°C$. (b) in the dark and with a light intensity of 5 mW/cm^2.

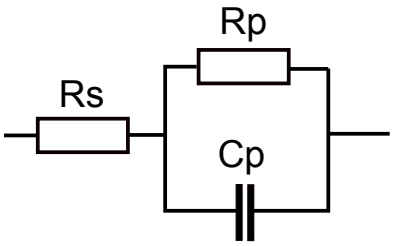

Figure 3.11: Equivalent circuit model for P3HT device

$$Z = Rs + \frac{1}{Rp^{-1} + i\omega Cp} \tag{3.1}$$

To simulate the equivalent circuit model one has to take equation 3.1. The simulated dots in figure 3.10 show the approximation to the specific measured dots, where the simulated dots are on the half circle. At 20 $°C$ in the dark the series resistance is Rs=40Ω, the parallel resistance Rp=117kΩ and the capacitor Cp is 1.5nF. The value of the capacitance refers to geometric capacitance from the electrodes. The series resistance reflects an ohmic behavior of the device, which is not dependent on temperature and light intensity. This are the resistances from the electrode to the measuring cables from the impedance meter. The highest contribution to

the series resistance in the device is the ITO electrode. The parallel resistance is the ohmic contribution from the film. It depends on the bias voltage, temperature and light intensity. In figure 3.10(a) the parallel resistance gets higher at lower temperatures. The same occurs by irradiating the device, but the effect is much higher with light. The parallel resistance Rp decreases from 117kΩ to 11kΩ with 5 mW/cm^2.

At a forward bias voltage of 1V, small illumination of 5 mW/cm^2 decreases the resistance of the film about a factor of 10. The resistance of the film also decreases with higher temperature.

3.4 Conductivity of P3HT films

In this section conductivity is measured and calculated with the P3HT device, introduced in section 2.1.5 and measured in the cryostat (2.2.2).

3.4.1 IV behavior in P3HT device

Following IV curves show the function of a device. In figure 3.12(a) the IV curve from the further used P3HT Schottky device and in (b) the modified 4 wire measurement resistance is shown. The linear IV behavior in figure (b) is a requirement for the 4 wire measurement, since it reflects a constant resistance over the whole voltage range.

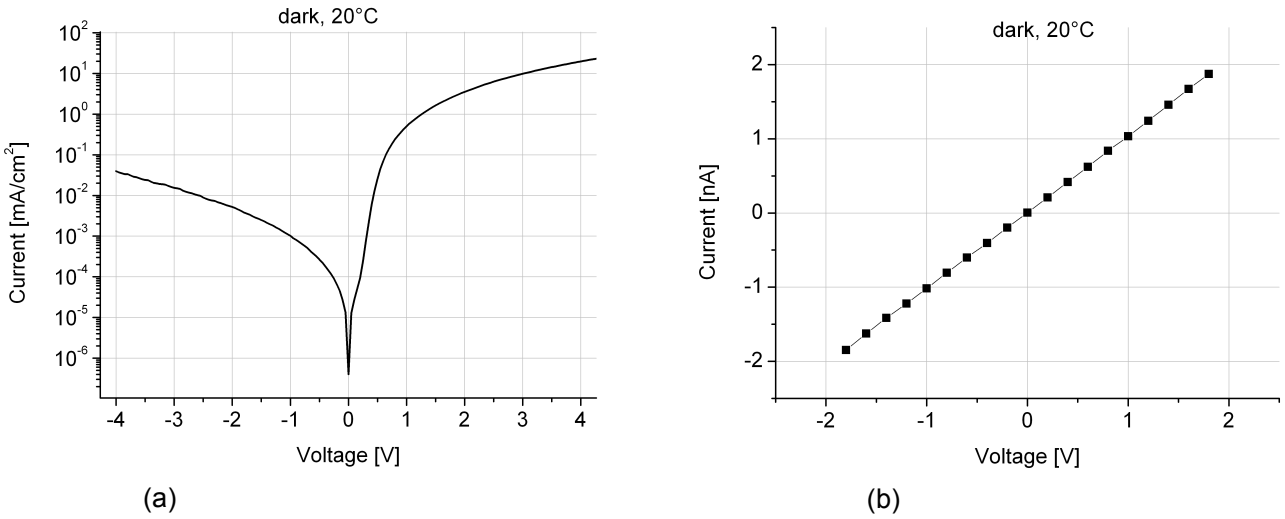

Figure 3.12: IV curves of P3HT device. (a) Schottky diode. (b) IV curve from modified 4 wire measurement

3.4.2 Conductivity in P3HT device

To measure the conductivity the modified 4 wire measurement is used, because contact resistance, specially in temperature dependent measurements, can affect the absolute conductivity. To measure the resistance (figure 3.13) at each temperature point and light intensity 4 IV points were measured and interpolated with a linear curve. The slope of the interpolated line is the resistance. The four points of all lines have good linear behavior, which is a requirement for a resistance measurement.

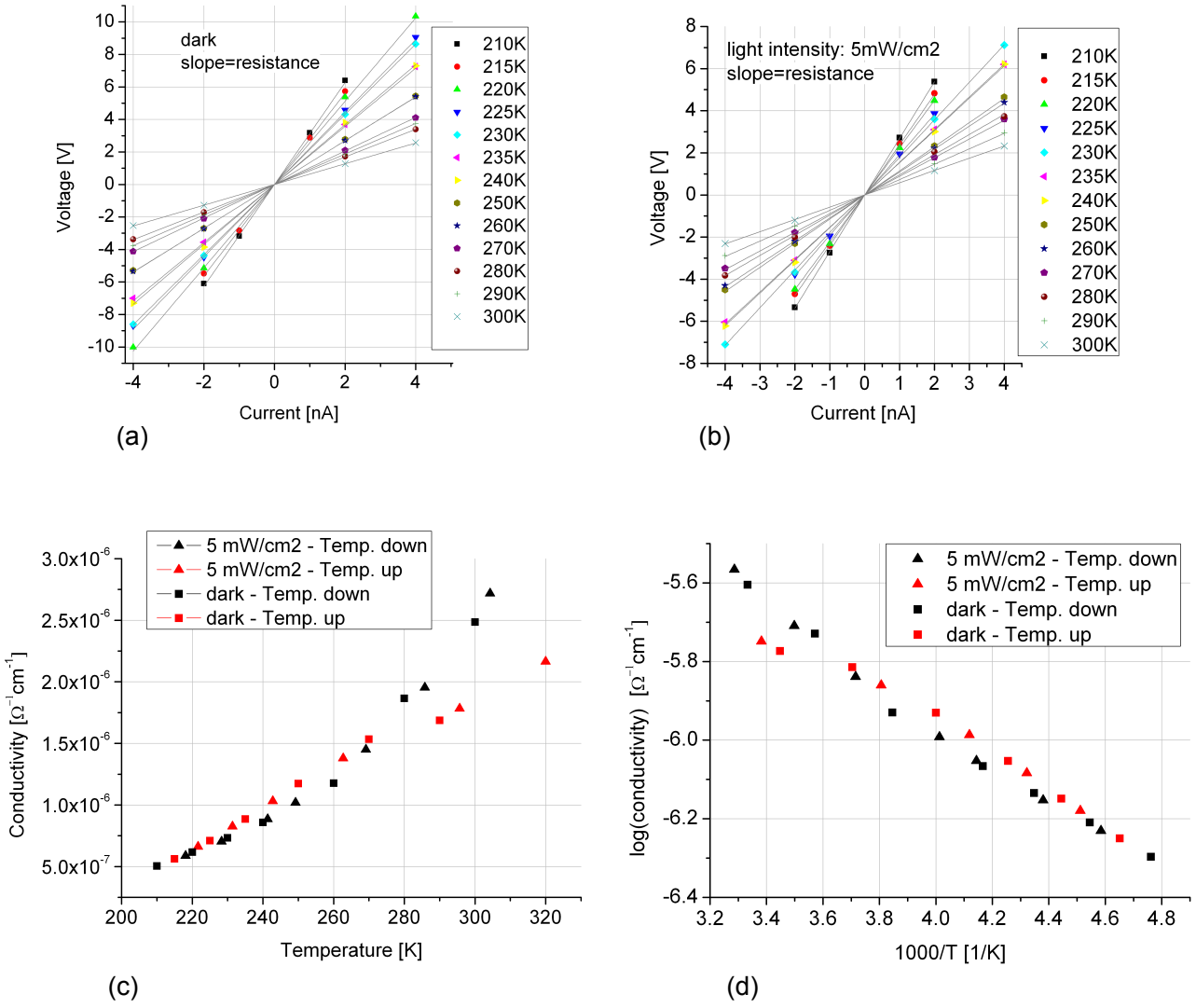

Figure 3.13: IV curves of modified 4 wire measurements in the dark (a) and at 5 mW/cm^2 light intensity (b). The slopes of the lines reflect the resistance at a certain temperature. (c) shows the conductivity dependence on the temperature of the P3HT device. (d) Arrhenius plot of the conductivity

Using equation (2.2) and the following device dependent results, one can calculate the conductivity of the device. The black points in figure 3.13(c) refer to measuring points by decreasing the temperature down to 210 K. By increasing the temperature (red points), the trend does not coincide with measuring points from before. Thus, the device changed his properties during

the measurements. There is no difference in the conductivity in the dark and at 5 mW/cm^2 light intensity. This may occur, because the geometry of the 4 wire conductivity measuring setup is not a sandwich-type but a planar device, see figure 2.5. In the device both electrodes are ITO and thus there is no Schottky-contact. There is only the electric field, more or less homogeneous distributed over the film area with a length of about 0.5mm. Thus, the present electric field is not able to dissociate excitons. This means no additional charges can contribute to a higher conductivity by irradiance the film with 5 mW/cm^2 (equal to an irradiance power of 5 % sun).

The conductivity of a P3HT film increases with higher temperature and does not depend on illumination.

3.4.3 Comparison of conductivities in P3HT device

As we measured the mobility using CELIV (in section 3.2.1), carrier concentration using Mott-Schottky analysis (in section 3.3.2.1) and CELIV (in section 3.3.2.2), and conductivity directly (in section 3.4) over a temperature range from 210 K to 290 K at the same time and thus the same conditions of the device, we can calculate equation $\sigma = en\mu$. The calculated conductivity (σ) should match the measured conductivity. Figure 3.14 shows the result.

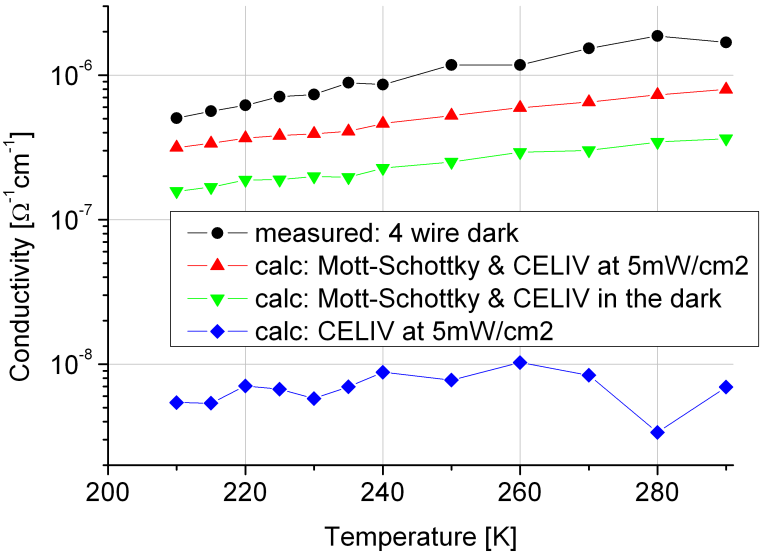

Figure 3.14: Measured and calculated conductivity in a P3HT device in the dark and at a light intensity of 5 mW/cm^2

The measured conductivity (black dots in figure 3.14) have an alternating noisy behavior. This comes from the change of the device during the measurement (see figure 3.13). This deviation

is not visible in the calculated curves. The calculated curves are based on the Schottky diode. The Schottky diode did not change during the measurement, possibly due to shielding of the semiconductor to the atmospheric conditions by the metal electrode.
At 210 K the measured conductivity is 2 to 3 times higher than the calculated conductivity. The calculated curve at 5 mW/cm^2 is higher compared to the curve in the dark, because the charge carrier density doubles with 5 mW/cm^2 light intensity. At 290 K the error factor between calculated and measured conductivity is 2 to 5. The calculated curve with the mobility and the charge carrier concentration measured by CELIV (blue squares in figure 3.14) is about 100 times lower than the measured conductivity. This comes mostly from the 50 times lower charge carrier concentration measured with the CELIV technique.
This difference in the conductivities can have several sources. First, the geometry of the device to measure 4 wire resistance and the geometry of the Schottky diode are very different. In the Schottky diode the charges move perpendicular to the substrate, whereas the charges in the 4 wire setup move parallel to the substrate. The polymers in the P3HT can have preferences to orientate themselves with respect to the substrate. Usually the backbones of the polymer tend to crystallize parallel to the substrate. Thus, the conductivity in 4 wire measurement would be higher, which is the case. Due to the different geometry also the electric field is different. The electric field in the Schottky diode is about 3 orders of magnitude higher, because of the much lower distance between the electrodes. But after Poole-Frenkel-type law the mobility increases with higher electric field, thus the conductivity in the Schottky diode should be higher, but it is lower.
Another possible error could be the mobility determination by CELIV. The mobilities in CELIV were higher if the laser was not in use. But, due to the low charge carrier concentration in P3HT the visible peak in CELIV was difficult to define. This would mean that the photo generated charges do not have the same mobility as the intrinsic charges. Further, as soon charges are photo-generated in the film, the diffusion current may contribute to the drift current. But the used equation for the mobility (1.9) is only based on the drift current, this could be an additional error.

Measuring the conductivities at different temperatures give 2 to 5 times higher conductivities than calculating the conductivities by determining the mobility with CELIV and the charge carrier concentration by the Mott-Schottky plot. Because the mobility is higher at higher temperatures, the conductivity also increases with higher temperature. The low charge carrier concentration from CELIV gives a 2 orders of magnitude lower conductivity.

3.5 P3HT film measurement summary

The mobilities, measured by CELIV and SCLC are listed in table 3.2. The mobility of the charge carriers in a P3HT film is higher with higher temperature. This can be seen between 20 $°C$ and -30 $°C$. But also with a light intensity of 100 mW/cm^2 the film gets warm, and shows a higher mobility. Mobility measured by SCLC and CELIV gives similar results and the same trends, regarding temperature dependence. The measured mobility in the device for the cryostat is higher than in the device for the small chamber. The production procedure is the

same, except the final annealing step in the device from the small chamber was accidentally not made. Annealing causes a higher cristallinity of the P3HT, which leads to a higher mobility. This may explain the 3 times higher mobility.
The charge carrier concentration in a P3HT device, see table 3.3, more than doubles with a small light intensity of 5 mW/cm^2, but by further increasing the light it stays more or less at the same value. The charge carrier concentration is not dependent on the temperature. The charge carrier concentrations from the different devices are similar. Thus, the annealing step does not affect the charge carrier concentration.

Mobilities	P3HT dark small chamber	P3HT $100mW/cm^2$ small chamber	P3HT dark cryostat
CELIV 20 $°C$ $[10^{-4}cm^2/Vs]$	1.3	1.7	3
CELIV -30 $°C$ $[10^{-4}cm^2/Vs]$	0.56	0.56	1.8
SCLC 20 $°C$ $[10^{-4}cm^2/Vs]$	2.7	-	-
SCLC -30 $°C$ $[10^{-4}cm^2/Vs]$	0.5	-	-

Table 3.2: Measured mobilities with small chamber and cryostat, dependent on light and temperature

Charge carrier concentration	P3HT dark small chamber	P3HT $5\,mW/cm2$ small chamber	P3HT $100mW/cm2$ small chamber	P3HT dark cryostat	P3HT $5\,mW/cm2$ cryostat
20 $°C$ $[10^{16}cm^{-3}]$	0.7	1.9	1.7	0.8	1.6
-30 $°C$ $[10^{16}cm^{-3}]$	0.97	1.9	2	0.8	1.6

Table 3.3: Measured charge carrier concentration with small chamber and cryostat, dependent on light and temperature

Overall the mobility, measured with different techniques, and charge carrier concentration show good and reproducible values and trends, regarding temperatures and illumination behavior. Where the used techniques, except the charge carrier concentration measurements by CELIV, show a good consistency with the conductivity measurements.

Chapter 4

Behavior of P3HT:PCBM bulk-heterojunction films

4.1 IV behavior in P3HT:PCBM films

In this section IV measurements with the BHJ device, introduced in section 2.1.4, measured in the the small chamber (2.2.1) are shown. The IV curves (figure 4.1) show temperature and light dependent behavior. The higher the light intensity, the higher the current in reverse bias, since more photo-generated charge carriers are available to participate in the current. At lower temperatures the dark current and the current in forward bias is lower.

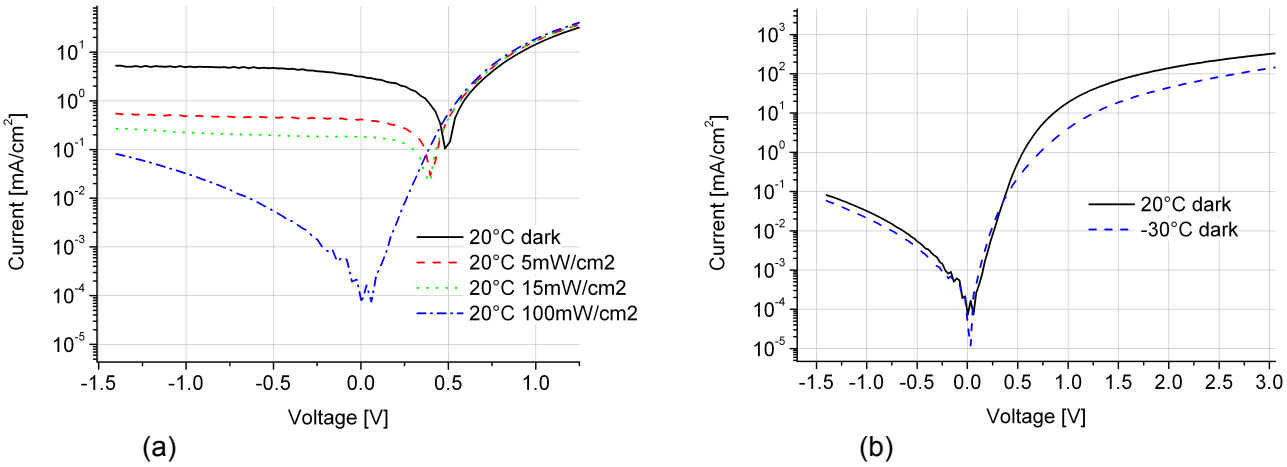

Figure 4.1: IV curves of a BHJ solar cell. (a) different light intensities. (b) different temperatures

In figure 4.2 the mobility is calculated with the Mott-Gurney relation (1.1). At -30 $°C$ and at 20 $°C$ the mobility is slightly lower with an illuminated film compared to the dark.
With higher temperature the mobility gets higher. This is visible in the dark and with a white

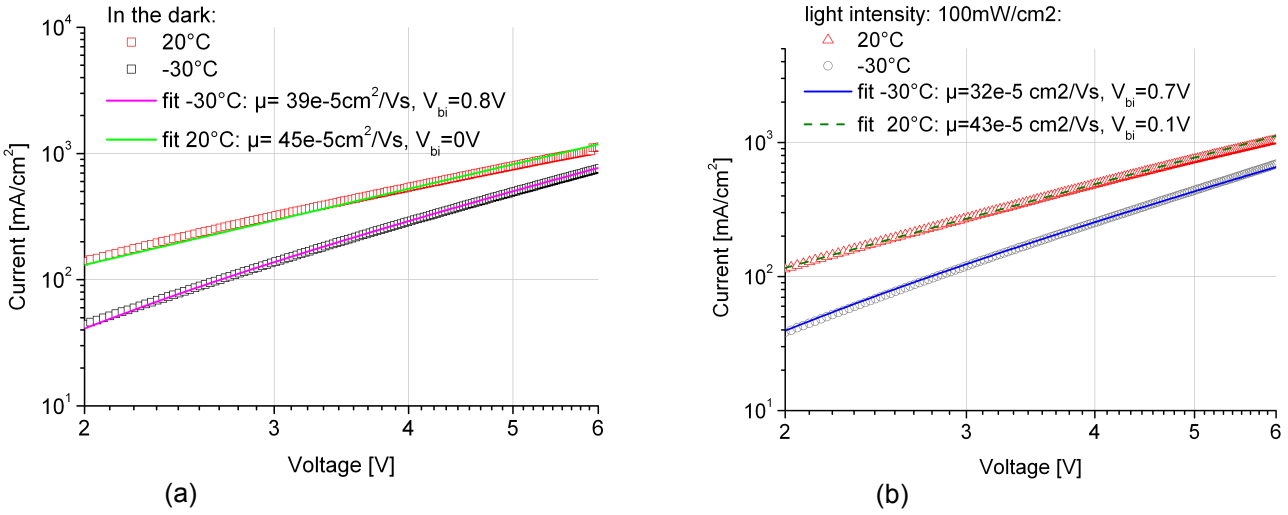

Figure 4.2: IV curve in space charge limited current regime and specific calculated mobility. (a) in the dark. (b) with 100 mW/cm^2 light intensity

light intensity of 100 mW/cm^2.

4.2 Mobility in P3HT:PCBM films

4.2.1 Mobility dependence on temperature

In this section mobility is measured and calculated with a P3HT-PCBM device (introduced in section 2.1.6). The device is measured in the cryostat (2.2.2), and the mobility will be used to calculate to conductivity in section 4.4.3.

The mobility of the charge carriers is measured by CELIV. In figure 4.3(a) the current transients in the dark are shown. The higher the temperature, the more mobile charge carriers are available and thus the peak is better recognizable. At 220 K the peak is very low and in this plot, it is difficult to define the time from the peak (t_{max}), but with a higher zoom the peak can be defined. In figure 4.3(b), the illuminated film keeps the charge carrier concentration on a certain level and therefore the peaks are good recognizable, also at low temperatures. The CELIV transient in a P3HT-PCBM device represents the sum of the extracted electrons and the extracted holes. Thus, the measured peak t_{max} gives the mobility somehow averaged between the mobilities of the two materials.

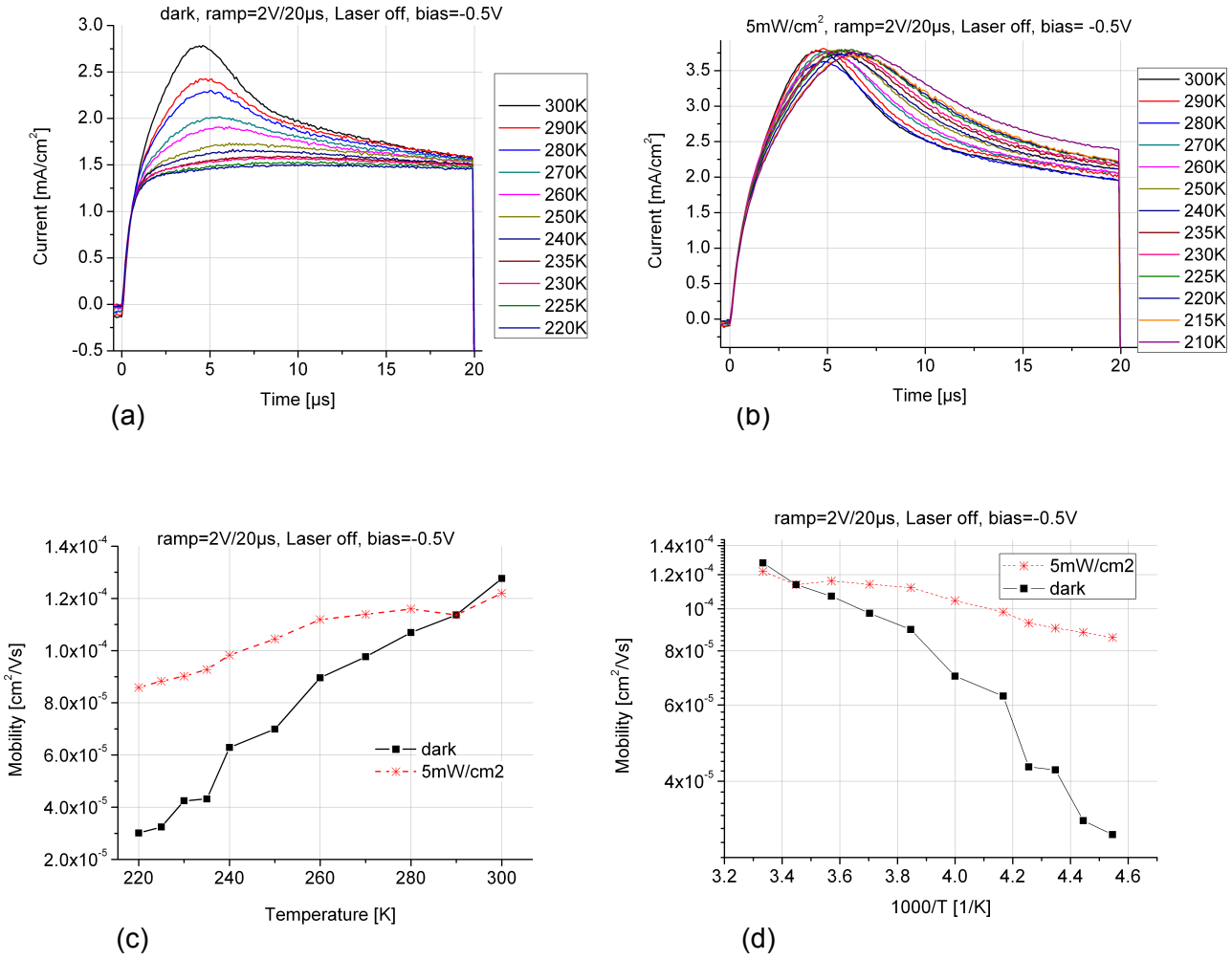

Figure 4.3: CELIV measurements on organic solar cell in the dark (a) and with irradiance of 5 mW/cm^2 (b). Calculated mobility at different temperatures in linear scale(c) and in the Arrhenius plot(d).

In figure 4.3(c) and 4.3(d) the mobility is calculated by equation 1.9. In 4.3(c) the mobility in the dark and at 5 mW/cm^2 is shown temperature dependent. The mobility at room temperature has about the same value. At 220 K the mobility is 3 times higher with an illumination of 5 mW/cm^2 compared to the mobility in the dark. This may come from the dependence of the mobility on the charge carrier concentration. The higher charge carrier concentration (the bump under the curve) induces a higher mobility. At room temperature this difference is not visible anymore, this means, the contribution of the thermal generated charges at room temperature is higher than the photo-generated charges at an irradiance of 5 mW/cm^2.
The noise or zig-zag behavior of the dark mobility curve comes from a change of the device during the measurements. The temperature measurements were done in the order: 300 K, 280 K, 260 K, 240 K, 230 K, 220 K, 225 K, 235 K, 250 K, 270 K, 290 K.

The higher the temperature the higher the mobility. Irradiance increased the mobility if the temperature is below 290 K.

4.2.2 Mobility dependence on illumination intensity

For the CELIV mobility measurements, the BHJ device (introduced in section 2.1.4) was used, which was measured in the the small chamber (2.2.1). As already mentioned, in the CELIV transient the measured t_{max} represents an averaged mobility of the holes and electrons of P3HT and PCBM.
Measuring the P3HT device, gives higher mobilities at higher temperatures. The mobilities in the solar cell (figure 4.4) have a similar temperature behavior. Higher temperature induces higher mobilities. Except in the dark, the mobility stays at $1.2 \cdot 10^{-4} cm^2/Vs$ at -30 $°C$ and 20 $°C$. The mobility also decreases with higher irradiance, this can not be a temperature effect like in the P3HT device, because with higher irradiance the temperature should be higher and thus the mobility higher. Therefore illumination does affect the mobility of the charge carriers in the device.

It has been theorized that increasing the charge carrier concentration will fill the low lying states, allowing for easier hopping dynamics [17]. The mobility is expected to increase with higher carrier concentration. Figure 4.4 shows the measured data have an opposite trend, which may be due to the limits of the validity of equation 1.9 when Δj is larger than $j_{(0)}$.

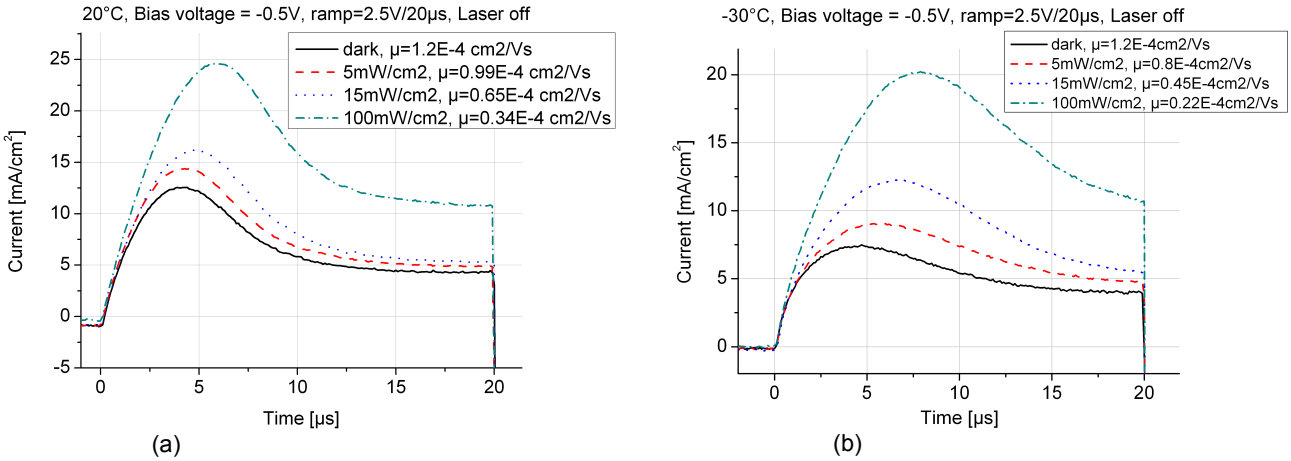

Figure 4.4: CELIV transients to measure mobility at different light intensities. (a) at 20 $°C$ and (b) at -30 $°C$

4.2.3 RC time constant in CELIV measurement

In CELIV measurement a voltage ramp is applied on a device and the current response is measured time dependent. In this section we calculate the influence of the RC contribution during the measurement. RC means a series connection of resistor and capacitor. By applying a ramp voltage on a RC circuit, the current response needs some time to keep up with the derivative of the voltage ramp. The time until the current could respond to the voltage ramp can be calculated. $\tau = RC$, where τ is the so called time constant in unit seconds, R the resistor and C the capacitor. After the time of τ the current has reached 63.2 % of his final value, and after 5τ the current has reached 99.3 % of his final value. Usually in electronic

circuits one says, is the system slower than 5τ, then there is no time dependent contribution from the RC circuit. The time 5τ for the used CELIV setup by measuring an organic solar cell will be calculated in this section.

In according to the film thickness of 160 nm the geometric capacitance is 1.83 nF. Rs contains the series resistance of the device and the internal resistance of the oscilloscope, which is 50 Ω. The series resistance of the device can be measured at high frequencies with impedance spectroscopy and is 27 Ω (not shown in this thesis). Based on this results we get:

$5\ \tau = 5RC = 5 \cdot (27 + 50)\Omega \cdot 1.83nF = 0.7\mu s$

The time for the current response from zero to the maximum in an equivalent capacitor takes about 0.7 μs. The CELIV transient is 20 μs long and the peak (t_{max}) usually between 2 μs and 5 μs. Thus RC does not affect significantly the t_{max} value, which is used to calculate the mobility.

4.3 Charge carrier concentration in P3HT:PCBM films

4.3.1 Charge carrier concentration dependence on temperature

In this subsection the P3HT-PCBM device introduced in section 2.1.6 is used. The device is measured in the cryostat (2.2.2), and the charge carrier concentrations will be used to calculate to conductivity in section 4.4.3.

The Mott Schottky plot, in figure 4.5(a), shows the capacitance behavior of a solar cell. The higher the bias, the higher the capacitance, since the depletion layer gets smaller. The lines are approximations to the points in the slope of the Mott Schottky plot. A slope of a line is inversely proportional to the charge carrier concentration. With equation 1.8, one can calculate the charge carrier concentration.
Figure 4.5(b) shows the calculated charge carrier concentration at different temperatures in the dark and with an irradiance of 5 mW/cm^2. In the dark and under illumination the charge carrier concentration gets lower with higher temperatures. Although in CELIV an opposite dependence of the charge carrier concentration on the temperature was recognized, see chapter 4.2.1, where the area under the bump gets higher with higher temperatures. The charge carrier concentration at 5 mW/cm^2 irradiance is about 10 times higher than in the dark in the whole measured temperature range.

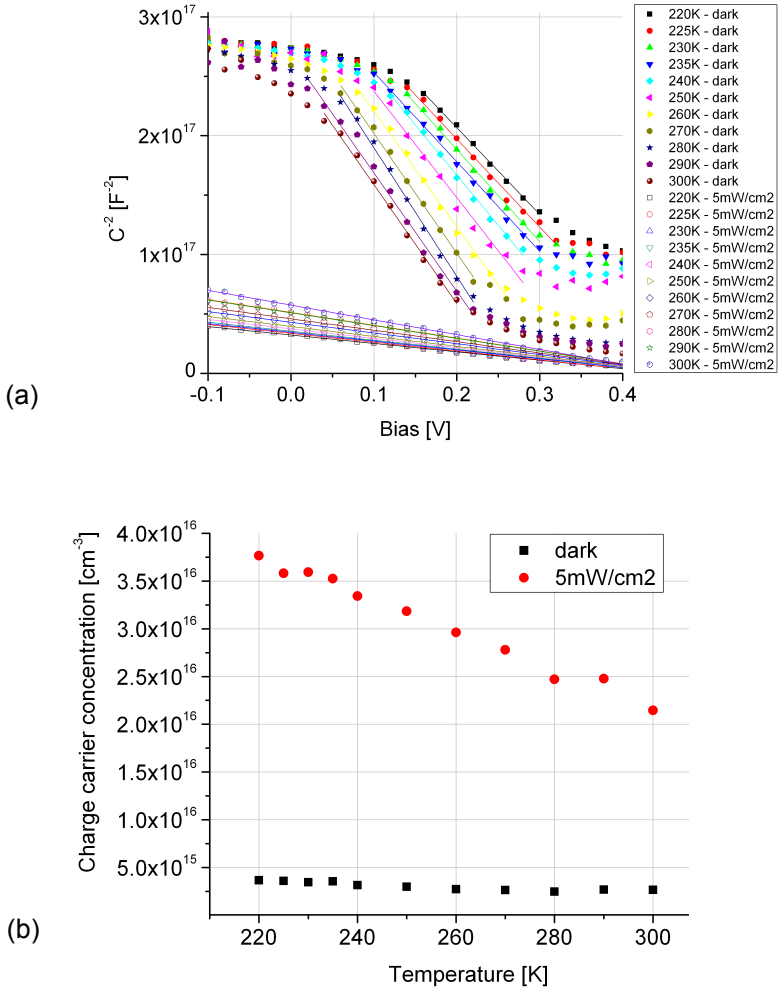

Figure 4.5: Mott Schottky plot of a P3HT-PCBM solar cell (a) in the dark and at 5 mW/cm^2. The calculated charge carrier concentrations (b) at different temperatures and light intensities.

Comparing the charge carrier concentrations of the solar cell with the P3HT device, one can see at 5 mW/cm^2 light intensity the P3HT device (figure 3.6) has a lower charge carrier concentration compared to the solar cell, but in the dark the charge carrier concentration is higher in the P3HT device than in the solar cell. With illumination the charge carriers can be separated at the junction and thus the solar cell has a higher charge carrier concentration. In the dark it is not clear, why the charge carrier concentration is smaller in solar cell than in the P3HT device. One can assume, that in the dark the charges in a P3HT-PCBM device mainly are present in the P3HT. It is understandable that the charge carrier concentration in the dark would be lower by roughly a factor of 2, because a significant volume fraction of the bulk is occupied by PCBM.

The charge carrier concentration gets smaller with higher temperatures. 5 mW/cm^2 irradiance generates 10 times more charges than in the dark, and this factor is not temperature dependent.

4.3.2 Charge carrier concentration dependence on light

In this subsection the measurements are made with the BHJ device introduced in section 2.1.4, measured in the the small chamber (2.2.1).

The interest in this subsection is to investigate the charge carrier concentration in an organic solar cell at different light intensities. In figure 4.6(a) and 4.6(b) the Mott-Schottky plots are visible with a linear approximation and at different temperatures. From this two plots, one can calculate built-in potential and charge carrier concentration, which is summarized in figure 4.6(c). The charge carrier concentration is lower at higher temperatures, and gets higher with illumination.

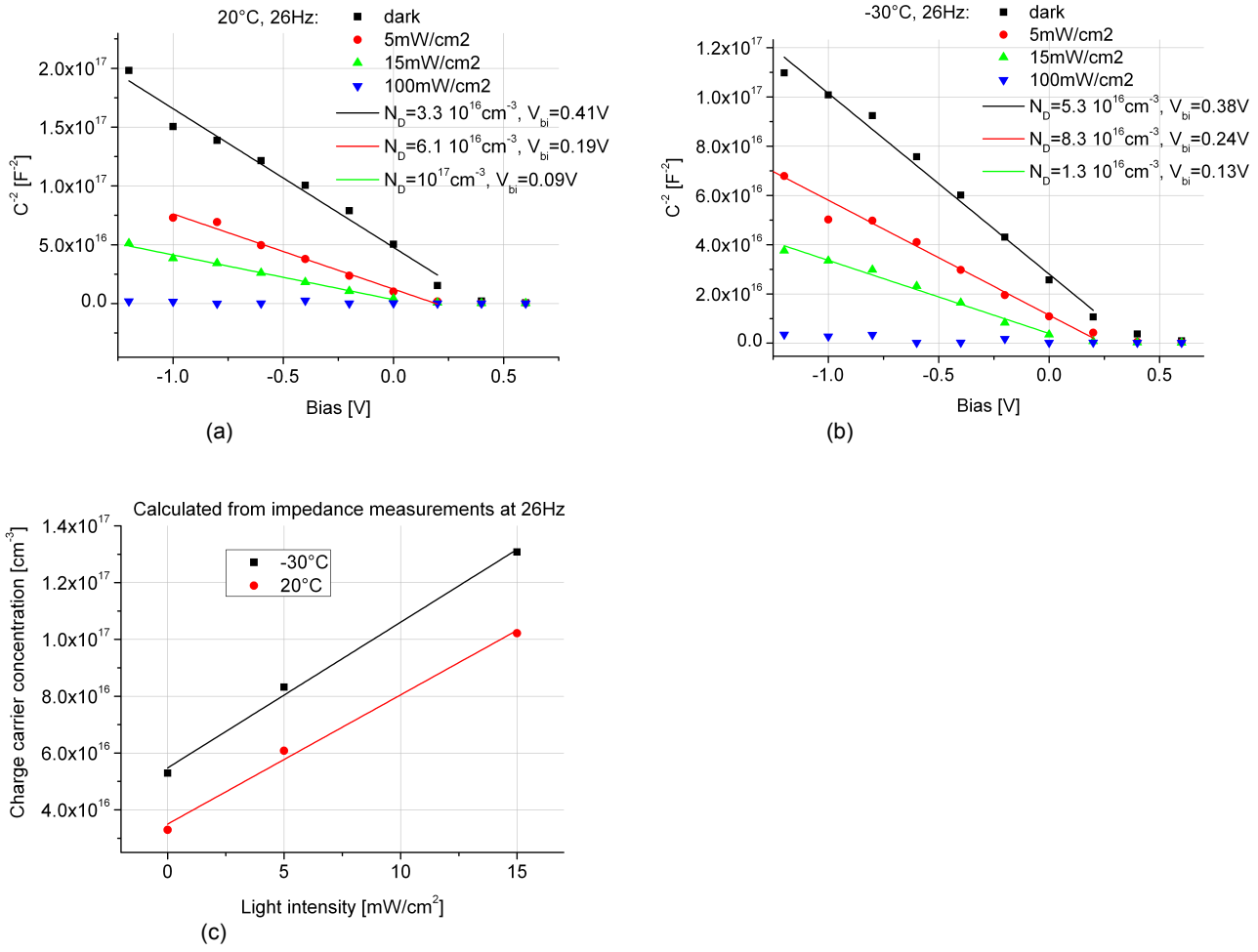

Figure 4.6: Charge carrier concentration measurements by impedance at different irradiances and temperatures. (a) Mott-Schottky plot at 20 °. (b) Mott-Schottky plot at -30 °. (c) Charge carrier concentration dependency of irradiance

4.3.3 Depletion layer thickness dependencies

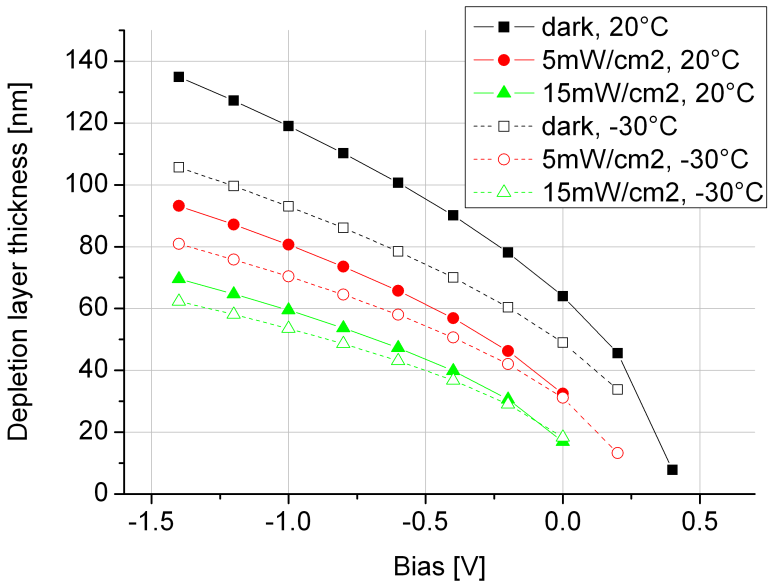

Figure 4.7: Depletion layer thickness over bias voltage in a P3HT-PCBM organic solar cell at different temperatures and irradiance.

After equation 1.5 the depletion layer thickness depends on the built-in potential and the charge carrier concentration. The depletion layer thickness is shown in figure 4.7. At a voltage of 0.3 V, which reflects the maximum power point of the IV curve, the thickness of the depletion layer under illumination is zero. At -1.6 V in all conditions the depletion layer does not expand over geometric film thickness of 160 nm, yet. The higher the irradiance, the higher the charge carrier concentration and thus the smaller the depletion layer. Also, due to higher charge carrier concentrations at lower temperatures the depletion layer gets smaller.

At 0.3 V the thickness of the depletion layer in the film under illumination is almost zero. Thus, in a solar cell the bulk is not affected by the high electric field from the depletion layer. This supports the idea, that the charge transport in an organic solar cell may not be affected by the electric field of the depletion layer and thus could be diffusion dominated, which is still under discussion.

4.4 Conductivity of P3HT:PCBM films

In this section conductivity is measured and calculated with a P3HT-PCBM device (introduced in section 2.1.6), which is measured in the cryostat (2.2.2).

4.4.1 IV behavior in P3HT:PCBM device

The IV curve is shown first, to give information about working range of the device. Under illumination of one sun, the solar cell has a short circuit current of 4.4 mA/cm^2, and open circuit voltage of 0.58 V.

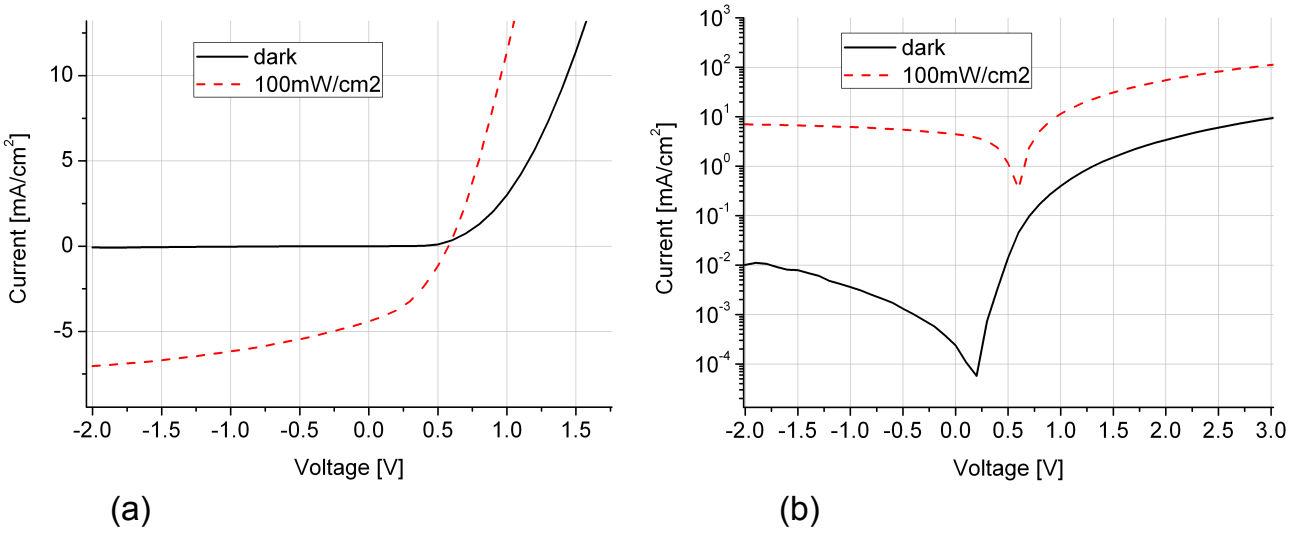

Figure 4.8: IV curves of P3HT-PCBM solar cell. (a) Linear scale. (b) Logarithmic scale

4.4.2 Conductivity in P3HT:PCBM device

The conductivity in the P3HT-PCBM device is measured with the modified 4 wire technique (see figure 2.5 and device geometry 2.1.6). This has been done at different temperatures, in the dark and with an irradiance of 5 mW/cm^2. In figure 4.9(a) the voltage-current diagram is shown. Since the resistance should have a ohmic behavior, the measured points can be connected with a linear line. The slope of the line gives the resistance at the specific temperature. In figure 4.9(b) the same is shown, but with illumination. The voltage is still positive at zero current. This means, in the second quadrant the device works as a solar cell. This is surprising, because the device is symmetric regarding used contact metals (see figure 2.5). There must be some unsymmetrical geometry which forces the separated charges to be collected rather at one electrode than at the other. The measured voltage still has a linear dependence on the current, thus the slope still gives the resistance.

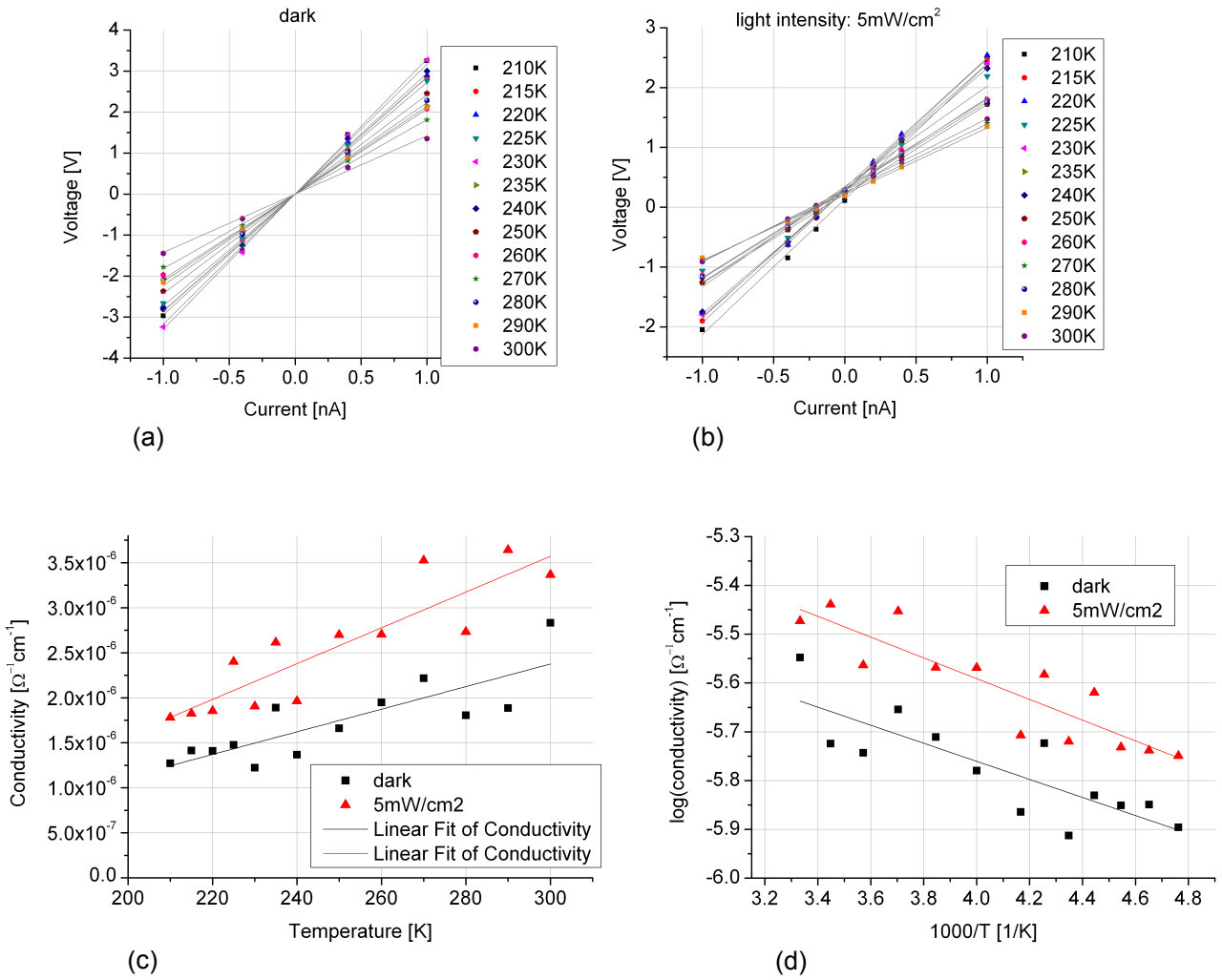

Figure 4.9: Modified 4 wire conductivity measurement on bulk heterojunction device in the dark (a) and at 5 % sun (b). Calculated conductivities at different temperatures and illuminations (c). (d) Arrhenius plot of the conductivity.

The conductivity is calculated with the geometric information from chapter 2.1.6. In figure 4.9(c) the results are shown temperature and light dependent. At 5 mW/cm^2 the average conductivity is about 50 % higher than in the dark, because the photo-generated charges can contribute to the current. In the dark and under illumination, with increasing temperature a trend of increasing conductivity is recognizable. Overall the noise of the calculated signal is high. Since the IV curve have a good linear behavior the device for the modified 4 wire measurements changes due to unknown reasons.

The conductivity gets higher with higher temperatures and with illumination of 5 mW/cm^2. The conductivity in the P3HT-PCBM device and in the P3HT device is similar.

4.4.3 Comparison of conductivities in P3HT:PCBM device

As we measured the mobility using CELIV (in section 4.2.1), carrier concentration using Mott-Schottky analysis (in section 4.3.1), and conductivity directly (in section 4.4.2) over a temperature range from 215 K to 300 K at the same time and thus the same conditions of the device, we can calculate equation $\sigma = en\mu$. The calculated conductivity (σ) should match the measured conductivity. Figure 4.10 shows the result.

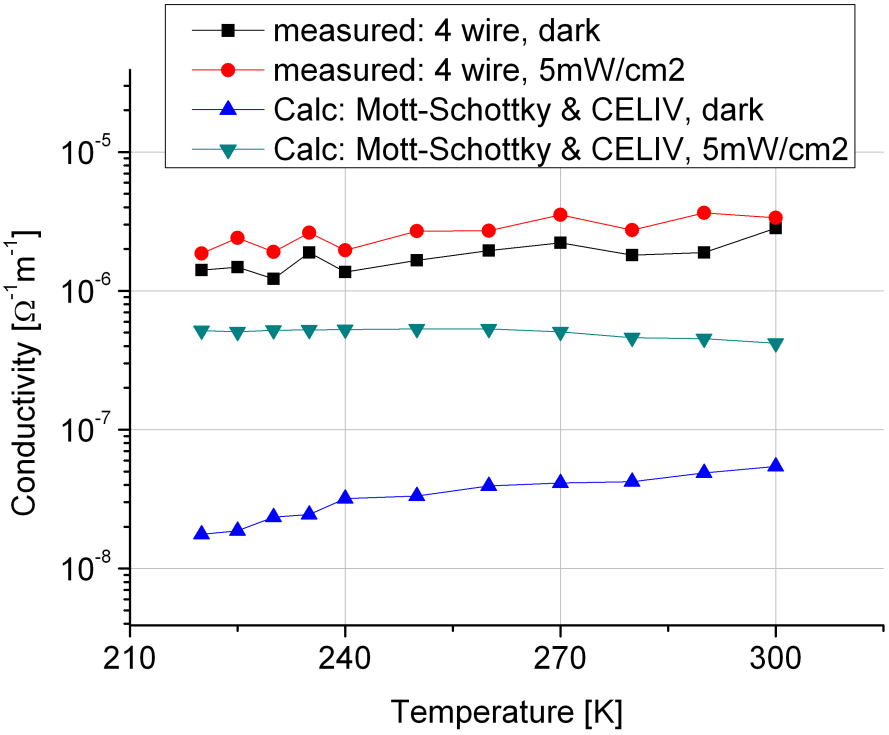

Figure 4.10: Measured and calculated conductivities from P3HT-PCBM heterojunction device at different temperatures, in the dark and under a light intensity of 5 mW/cm^2.

The circle and the squares in figure 4.10 represent the measured conductivity, which is similar to the measured conductivity in pure P3HT (see 3.14). But here in the P3HT-PCBM device a clear difference between the measured conductivity in the dark and under illumination is recognizable. The measured conductivity under illumination is about 2 times higher. This could come from a higher charge carrier concentration, shown in figure 4.5. The calculated curve at 5 mW/cm^2 at 220 K is about 3 times smaller and at 300 K about 7 times smaller than the measured conductivity. The mismatch gets bigger in the dark, where the calculated conductivity is 50-80 times lower than the measured conductivity.
At 290 K the conductivities of the P3HT device and the BHJ device is similar. But the charge carrier concentration and the mobility in the P3HT-PCBM device is about 3 times lower at 290 K than in the P3HT device. Thus the lower charge carrier concentrations and the lower mobilities contribute to the mismatch between the measured and calculated conductivities. The reason of the mismatch requires more investigation.

In the conductivity measurements holes may dominate the charge transport, since the 2 ITO electrodes make a quasi ohmic contact to the HOMO of the P3HT. Whereas the PCBM as a electron conductor has a higher LUMO level than the ITO work function, and thus can not contribute to the charge transport in the dark.

The mismatch between calculated and measured conductivities is higher than in the P3HT device. In the dark the lower charge carrier concentration and the lower mobility is responsible for the 50-80 times lower conductivity. With a light intensity of 5 mW/cm^2 the calculated conductivity is 3 to 7 times too low.

4.5 P3HT:PCBM film measurement summary

The mobilities, measured by CELIV and SCLC are listed in table 4.1. In all conditions, higher temperature induces an equal or higher mobility. Mobility measured by SCLC shows similar trends like the mobility measured by CELIV. But the changes in the mobility due to different light intensities are higher in the CELIV mobility.

Mobilities	BHJ dark small chamber	BHJ $100mW/cm^2$ small chamber	BHJ dark cryostat	BHJ 5 mW/cm^2 cryostat
CELIV 20 $°C$ $[10^{-4}cm^2/Vs]$	1.2	0.34	1.1	1.1
CELIV -30 $°C$ $[10^{-4}cm^2/Vs]$	1.2	0.22	0.6	1
SCLC 20 $°C$ $[10^{-4}cm^2/Vs]$	4.5	4.3	-	-
SCLC -30 $°C$ $[10^{-4}cm^2/Vs]$	3.9	3.2	-	-

Table 4.1: Measured mobilities with small chamber and cryostat, dependent on light and temperature

Charge carrier concentration	BHJ dark small chamber	BHJ 5 mW/cm^2 small chamber	BHJ $15mW/cm^2$ small chamber	BHJ dark cryostat	BHJ 5 mW/cm^2 cryostat
20 $°C$ $[10^{16}cm^{-3}]$	3.3	6.1	10	0.3	2.1
-30 $°C$ $[10^{16}cm^{-3}]$	5.3	8.3	13	0.4	3.3

Table 4.2: Measured charge carrier concentration in solar cells with small chamber and with cryostat, dependent on light and temperature

In the bulk heterojunction solar cell, the charge carrier concentration increases with a higher light intensity, due to the charge separation behavior of an organic solar cell (see table 4.2). Currently, the understanding for organic charge transport predicts a higher mobility at higher temperatures, and with higher charge carrier concentration the mobility should also be higher. In the solar cell measured in the cryostat this is the case. But in the solar cell measured in the small chamber the illumination behavior is opposite. The only difference in production of the

devices is, the solar cell for the cryostat was spin coated inside the glovebox, whereas the solar cell for the small chamber was spin coated outside the glovebox and thus more oxygen doping may affect the device. Also, the charge carrier concentration from the small chamber solar cell is higher than from the device for the cryostat (see table 4.2). Based on this, oxygen doping could affect the behavior of the mobility in a BHJ solar cell. Also reported here [18].

Chapter 5

Conclusions

By using 5 different techniques, the charge carrier concentration, carrier mobility, and overall conductivity of P3HT and P3HT:PCBM systems have been investigated. The specific dependencies on background illumination and temperature have been explored. The various techniques give differing values, but show surprisingly good agreement for the wide range of experimental conditions used. Furthermore, the trends with temperature and illumination are consistent with a few exceptions.

The mobilities measured by CELIV and SCLC give similar results in a P3HT device. The mobility in a P3HT device gets higher with increasing temperature. Permanent illumination does slightly increase the mobility. The increase of the mobility due to illumination may come from an increasing temperature in the film. It has been recognized that a P3HT device under illumination at 20 $°C$ and with a previous laser pulse, for the CELIV technique, has a lower mobility than the same system without the laser pulse. Assuming no temperature effect from the laser pulse, the decrease may come from a higher charge carrier concentration.
By using a bias voltage, which minimizes the extracted charges before the voltage ramp, the mobility does not depend on the slope of the ramp.

The charge carrier concentration, measured by CELIV, in the P3HT device depends exponentially on the bias voltage. This gives rise to the assumption, that with CELIV one measures not only the intrinsic carriers but also the injected carriers. CELIV is not the appropriate technique to measure intrinsic charge carrier concentration in low conductive materials, because with zero bias no visible charges are extracted and with a bias one extract the injected charge carriers.

Measured by impedance, the charge carrier concentration in a P3HT device does not depend on the temperature. But the charge carrier concentration more than doubles with a small white light intensity of 5 mW/cm^2. By further increasing the light, the concentration stays more or less at the same value. Since we do not have an acceptor, charges should not be generated. But charges can also be photo generated at impurities or at the junctions to the electrodes. By further increasing the light, no additional charges are generated anymore. It seems that a light intensity of 5 mW/cm^2 already saturates the possible amount of photo generated charges. This effect is visible at 20 $°C$ and at -30 $°C$.

Using impedance spectroscopy by measuring the P3HT device, the approximation of the impedance in the Nyquist plot can be done with one half circle. This half circle refers to the geometric capacitance of the device. At a forward bias voltage of 1 V, small illumination of 5 mW/cm^2 decreases the parallel resistance of the equivalent circuit model 10 times. In the measured range, the resistance of the film also decreases with higher temperature.

The conductivity of a P3HT film increases with higher temperature. It does not depend on illumination, because the generated excitons can not dissociate, since there is no acceptor molecule in a pure P3HT film. Measuring the conductivities between 210 and 290 K gives 2 to 5 times higher conductivities than calculating the conductivities with relation $\sigma = en\mu$, by determining the mobility with CELIV and the charge carrier concentration by the Mott-Schottky plot. Because the mobility is higher at higher temperatures, the calculated conductivity also increases with higher temperature even though the carrier concentration remains relatively constant. The low charge carrier concentration from CELIV gives a 2 orders of magnitude lower conductivity.

The mobilities in the bulk heterojunction solar cell, measured by CELIV and SCLC, are higher or equal at 20 $°C$ compared to -30 $°C$. Mobility measured by SCLC shows similar trends like the mobility measured by CELIV. But the changes in the mobility due to different light intensities are higher in the CELIV mobility.
Currently, the understanding for organic charge transport predicts a higher mobility with higher temperatures and also with higher charge carrier concentrations. In the solar cell measured in the cryostat this is the case. But in the solar cell measured in the small chamber the illumination behavior is opposite. The only difference in production of the devices is, the solar cell for the cryostat was spin coated inside the glovebox, whereas the solar cell for the small chamber was spin coated outside the glovebox and thus more oxygen doping may affect the device. Also, the charge carrier concentration from the small chamber solar cell is higher than from the device for the cryostat. Based on this, oxygen doping could affect the behavior of the mobility in a BHJ solar cell. Also reported here [18].

In the P3HT-PCBM device, the charge carrier concentrations gets higher with increasing light intensities. But, the charge carrier concentration gets smaller with higher temperature. At 0.3 V bias, and thus at the maximum power point of the solar cell, the thickness of the depletion layer in the film under illumination is zero. Thus, in a solar cell the bulk is not affected by the high electric field from the depletion layer. This supports the idea, that the charge transport in an organic solar cell may not be affected by the electric field of the depletion layer and thus could be diffusion dominated, which is still under discussion.

Between 215 and 300 K, the measured conductivity in a solar cell gets higher with higher temperatures and with an illumination of 5 mW/cm^2. The measured conductivity in the P3HT-PCBM solar cell and in the P3HT device is similar. The mismatch between calculated and measured conductivities is higher then in the P3HT device. With a light intensity of 5 mW/cm^2 the calculated conductivity is 3 to 7 times too low compared to the measured conductivity. In the dark the lower charge carrier concentration and the lower mobility is responsible for the 50-80 times lower calculated conductivity, thus in a solar cell either the measured conductivity is too high, or the measured mobility and charge carrier concentration is too low, or both.

5.1 Suggestions for further research

An interesting topic for further research would be, why the measured conductivity in an OPV device in the dark is 50 to 80 times different to the calculated one?
Based on the results, that the depletion layer thickness in a illuminated solar cell is zero, induces the question how the electric field is distributed in the film. After the Poisson equation (1.6) the electric field is the derivative of the potential. Thus, because an illuminated solar cell has a potential difference at the electrodes, there must also be an electric field in bulk. But how does it looks like?
Another interesting investigation would be to measure charge carrier concentration, mobility and conductivity of PCBM, to complete the picture beside the already measured P3HT and the P3HT:PCBM BHJ device. This was not done yet, because pure PCBM films are not easy to produce and need a supporting matrix, like polystyrene (PS). First trials with a PCBM:PS mixtures were partially successful, but electrically not very stable.
For further understanding of the physics in OPV devices, the recombination rate of the photo-generated charges could be measured at different permanent light intensities and temperatures. This can be done with the Photo-CELIV method, by changing the delay time of the Laser pulse.

Chapter 6

Appendix

6.1 list of abbreviations

HOMO = Highest occupied molecular orbital

LUMO = Lowest unoccupied molecular orbital

SCLC = Space charge limited current

PCBM = Phenyl-C61-butyric acid methyl ester

P3HT = Poly(3-hexylthiophene-2,5-diyl)

ITO = Indium tin oxide

CELIV = Charge extraction by linear increasing voltage

AFM = Atomic force microscope

BHJ SC = Bulk heterojunction solar cell

OPV = Organic photo voltaic

DOS = Density of states

Voc = Open circuit voltage

PS = Polystyrene

Bibliography

[1] C. Brabec, N. Sariciftci, and C. Hummelen, "Plastic solar cells," *Adv. Mater.*, vol. 11, pp. 15–26, 2001.

[2] H. Hoppe and N. Sariciftci, "Organic solar cells: An overview," *J. Mater. Res.*, vol. 19, pp. 1924–1945, 2004.

[3] J. Nakamura, K. Murata, and K. Takahashi, "Relation between carrier mobility and cell performance in bulk heterojunction solar cells consisting of soluble polythiophene and fullerene derivatives," *Appl.Phys. Lett.*, vol. 87, p. 132105, 2005.

[4] A. Campbell, D. Bradley, and H. Antoniadis, "Trap-free, space-charge-limited currents in a polyfluorene copolymer using pretreated indium tin oxide as a hole injecting contact," *Synth. Met.*, vol. 122, p. 161, 1955.

[5] A. Mozer, N. Sariciftci, A. Pivrikas, R. Oesterbacka, G. Juska, L. Brassat, and H. B"assler, "Charge carrier mobility in regioregular poly(3-hexylthiophene) probed by transient conductivity techniques: A comparative study," *PHYSICAL REVIEW B*, vol. 71, pp. 352141–352149, 2005.

[6] H. Michaelson, "Relation between an atomic electronegativity scale and the work function," *IBMJ*, 1978.

[7] C. Garrett and W. Brattain, "Physical theory of semiconductor surfaces," *Phys.Rev.99*, p. 376, 1955.

[8] A. Kavasoglu, N. Kavasoglu, and S. Oktik, "Simulation for capacitance correction from nyquist plot of complex impedance voltage characteristics," *Solid State Electronics*, vol. 52, p. 990, 2008.

[9] S. Sze and K. Kwok, *Physics of Semiconductor Devices*. Wiley - VCH, 2007.

[10] G. Juska, K. Arlauskas, M. Viliunas, and K. Genevicius, "Charge transport in p-conjugated polymers from extraction current transients," *Physical Review B*, vol. 62, 2000.

[11] A. Zen, J. Pflaum, S. Hirschmann, W. Zhunang, F. Kaiser, U. Asawapirom, J. Rabe, and D. N. U. Scherf, "Effect of molecular weight and annealing of poly(3-hexylthiophene)s on the performance of organic field-effect transistors," *Adv. Funct. Mater.*, vol. 14, p. 757, 2004.

[12] P. Schilinsky, U. Asawapirom, U. Scherf, M. Biele, and C. Brabec, "Influence of the molecular weight of poly(3-hexylthiophene) on the performance of bulk heterojunction solar cells," *Chem. Mater.*, vol. 17, p. 2175, 2005.

[13] D. Veldman, S. Meskers, and R. Janssen, "The energy of charge-transfer states in electron donor-acceptor blends: insight into the energy losses in organic solar cells," *Adv.Funct.Material*, vol. 19, pp. 1939–1948, 2009.

[14] T. Brown and et al. *Appl. Phys. Lett.*, vol. 75, p. 1679, 1999.

[15] G. Garcia-Belmonte, A. Munar, E. Barea, J. Bisquert, I. Ugarte, and R. Pacios, "Charge carrier mobility and lifetime of organic bulk heterojunctions analyzed by impedance spectroscopy," *Organic Electronics*, vol. 9, pp. 847–851, 2008.

[16] A. Campbell, D. Bradleya, and H. Antoniadis, "Trap-free, space-charge-limited currents in a polyfluorene copolymer using pretreated indium tin oxide as a hole injecting contact," *Synthetic Metals*, vol. 122, pp. 161–163, 2001.

[17] I. I. Fishchuk, A. Kadashchuk, J. Genoe, M. Ullah, H. Sitter, T. Singh, N. Sariciftci, and H. Baessler, "Temperature dependence of the charge carrier mobility in disordered organic semiconductors at large carrier concentrations," *Physical Rev.B*, vol. 81, p. 45202, 2010.

[18] J. Schafferhans, A. Baumann, A. Wagenpfahl, C. Deibel, and V. Dyakonov, "Oxygen doping of p3ht:pcbm blends: Influence on trap states, charge carrier mobility and solar cell performance," *Organic Electronics*, vol. 11, pp. 1693–1700, 2010.